Biochemical Pharmacology 239 (2025) 117037

Contents lists available at ScienceDirect

Biochemical Pharmacology

journal homepage: www.elsevier.com/locate/biochempharm

A mathematical formalism to quantify drug-target residence time

Antonio J. Ortiz [a,b,c], David Romero [e], Antoni Guillamon [d,e,*], Jesús Giraldo [a,b,c,*]

[a] Laboratory of Molecular Neuropharmacology and Bioinformatics, Unitat de Bioestadística and Institut de Neurociències, Universitat Autònoma de Barcelona, 08193 Bellaterra, Spain
[b] Instituto de Salud Carlos III, Centro de Investigación Biomédica en Red de Salud Mental, CIBERSAM, Spain
[c] Unitat de Neurociència Traslacional, Parc Taulí Hospital Universitari, Institut d'Investigació i Innovació Parc Taulí (I3PT), Institut de Neurociències, Universitat Autònoma de Barcelona, Spain
[d] Departament de Matemàtiques and IMTech, Universitat Politècnica de Catalunya, Barcelona, Spain
[e] Centre de Recerca Matemàtica, Universitat Autònoma de Barcelona, 08193 Bellaterra, Spain

ARTICLE INFO

Keywords:
Residence time
Binding kinetics
Receptor heterodimerization
Conformational selection
Induction fit
Constitutive receptor activity

ABSTRACT

Despite *drug-target residence time* (RT) is a key topic in binding kinetics, little information exists on its theoretical quantification. The two most frequent mathematical expressions found in the literature correspond to two particular and simple pharmacological cases: the binary ligand-receptor complex and the induction-fit model. In this article, we propose a mathematical formalism to obtain an expression of RT that can be of general applicability. RT is calculated from the system of ordinary differential equations (ODE) obtained by applying the Law of Mass Action to the selected chemical process. Then, a subsystem is constructed by defining which chemical species are of interest and omitting their global formation processes. RT maintains its accepted definition of $1/k_{off}$, where k_{off} is here defined as the absolute value of the smallest-modulus eigenvalue of the subsystem. The proposed procedure is successfully used to derive RT for a wide variety of pharmacological cases. In particular, the theoretical expressions of RT obtained for binary ligand-receptor binding and induction-fit coincide with those previously found in the literature. An extension of the RT pharmacological framework is proposed by including the concept of *relaxation time* (RXT), which involves pharmacological conditions associated with receptor activation rather than receptor binding. To conclude, the herein presented formalism for RT and RXT provides a mathematical framework that can be of general applicability in many pharmacological systems. It is expected that the procedure may be helpful in different pharmacological areas such as binding kinetics, PK/PD and enzymology.

1. Introduction

Residence time (RT) refers to the time span that a molecule or particle remains within a specific environment or system before exiting or undergoing/eliciting a transformation. In the context of binding kinetics, RT measures the duration or lifetime of the ligand-receptor complexed species and then it corresponds to the concept of drug-target residence time [1]. It is a critical parameter that influences the efficacy and duration of molecular interactions. Consequently, it influences the effectiveness of the drug's action, so that a longer residence time typically corresponds to greater therapeutic effectiveness.

The simplest case of ligand-receptor binding [2] is the formation/dissociation of a binary ligand-receptor complex (LR) involving a ligand L and a receptor R as represented in the following:

$$L + R \underset{k_{-1}}{\overset{k_1}{\rightleftarrows}} LR \tag{1}$$

Here, k_1 and k_{-1} are the rate constants of LR formation and LR dissociation, respectively, that is, the single microscopic rate constants directly involved in the ligand-receptor binding and unbinding processes. The Law of Mass Action establishes that the variation of LR concentration over time depends on the rates of LR formation (r_f) and LR dissociation

Abbreviations: CPA, N^6-cyclopentyladenosine; GPCR, G protein-coupled receptor; mAChR, Muscarinic acetylcholine receptor; MOR, μ-opioid receptor; MRT, Mean residence time; NAM, Negative allosteric modulator; NECA, N-5′-ethylcarboxamidoadenosine; NMS, N-methylscopolamine; ODE, Ordinary differential equation; PAM, Positive allosteric modulator; PK/PD, Pharmacokinetics/Pharmacodynamics; RT, Drug-target residence time; RXT, Relaxation time.

* Corresponding authors.
E-mail addresses: antoni.guillamon@upc.edu (A. Guillamon), Jesus.Giraldo@uab.es (J. Giraldo).

https://doi.org/10.1016/j.bcp.2025.117037
Received 7 November 2024; Received in revised form 25 April 2025; Accepted 5 June 2025
Available online 16 June 2025

(r_d) according to the following differential equation:

$$\frac{d[LR]}{dt} = r_f - r_d = k_1[L][R] - k_{-1}[LR]. \quad (2)$$

At equilibrium, association and dissociation rates are equal, that is, d[LR]/dt = 0, which leads to:

$$k_1[L]_{eq}[R]_{eq} = k_{-1}[LR]_{eq}, \quad (3)$$

and the ratio between k_{-1} and k_1 defines the equilibrium dissociation constant:

$$K_d := \frac{k_{-1}}{k_1} = \frac{[L]_{eq}[R]_{eq}}{[LR]_{eq}}. \quad (4)$$

Macroscopic dissociation and association rate constants are usually named k_{off} and k_{on}, respectively. For Eq. (1), $k_{off} = k_{-1}$ and $k_{on} = k_1$. For situations more convoluted than that represented by the binary ligand-receptor complex, k_{off} and k_{on} result in mathematical expressions that include a combination of microscopic rate constants.

RT is mathematically defined as the reciprocal of k_{off} and is denoted by τ [1]:

$$\tau = \frac{1}{k_{off}}, \quad (5)$$

which measures the affinity of the ligand for the receptor once it is occupied.

It is considered that RT is especially indicated as an efficacy measure for *in vivo* situations, which correspond to open systems in which the species involved are not in equilibrium [1]. However, the relationship between RT and efficacy is not limited to *in vivo* situations and can be found in all those situations in which a minimum time interval of ligand-receptor occupancy is necessary for signal transmission, for instance, for the binding of a transducer protein to the ligand-receptor complex [3]. To explicitly distinguish between receptor species unable or able of signal transmission, it is typical in receptor theory to include two ligand-receptor species: the inactive (LR) and the active one (LR*), that are exchanged reversibly:

$$L + R \underset{k_{-1}}{\overset{k_1}{\rightleftarrows}} LR \underset{k_{-2}}{\overset{k_2}{\rightleftarrows}} LR^* \quad (6)$$

In the case of G protein-coupled receptors (GPCRs), LR needs to undergo a conformational change to LR* to allow binding of the transducer G protein and to proceed through the signal transmission process. The probability of a G protein binding the ligand-receptor complex is dependent on the time interval of the receptor in the active LR* conformation. In this context, k_{off} and τ become combinations of the microscopic rate constants included in the receptor system (6). Indeed, the chemical process (6) appears frequently in the literature with its corresponding k_{off} and τ expressions [1]:

$$k_{off} = \frac{k_{-1}k_{-2}}{k_{-1} + k_{-2} + k_2}; \tau = \frac{k_{-1} + k_{-2} + k_2}{k_{-1}k_{-2}}. \quad (7)$$

It is worth noting that the expressions in (7) include all the rate constants in Eq. (6) except for k_1, the association rate constant between the ligand and the receptor.

The expressions in Eq. (7) have been obtained from different perspectives in the literature. In the appendix of this article, we examine two representative approaches developed by Kenneth Johnson (Appendix A) and Athel Cornish-Bowden (Appendix B), respectively [4,5]. In the first approach, a procedure to obtain k_{off} for chemical systems compatible with Eq. (6) is presented; more precisely, a ligand–protein complex formation followed by a conformational change of the complex. In the latter approach, although k_{off} was not calculated, the author provides a complete analytical solution of the time evolution of the concentrations of chemical species in a model of a sequence of two generic chemical reactions.

We would like to point out, on the one hand, that none of the above approaches explicitly mentions the term *residence time* and, on the other hand, that the chemical mechanisms involved in them are both equivalent to Eq. (6), although Johnson's approach is presented in the context of enzymatic reactions and Cornish-Bowden's in a more general context. This double example shows the ubiquity of reaction schemes across biochemical paradigms, but also a disparity in the methodology. Moreover, it is also true that for biological systems more complex than Eq. (6), it is not straightforward to find a general procedure to define k_{off}.

In the search for other approaches in the literature related to the concept of residence time in a pharmacokinetic context, we can mention the concept of *mean residence time* (MRT) [6,7]. Mathematically speaking, MRT is defined as the time that a drug is expected to last in a compartment. More precisely, if we define the probability density function

$$\phi(t) = \frac{\sum_{i=1}^{n} k_i x_i(t)}{\int_0^\infty \sum_{i=1}^{n} k_i x_i(t) dt}, \quad (8)$$

where $x_i(t)$ is the analytical expression for drug concentration in the i-th compartment and k_i is the corresponding rate of elimination from the compartment; MRT is defined as the mean value of the distribution (8):

$$MRT = \int_0^\infty t\phi(t)dt. \quad (9)$$

This concept can be also applied to binding kinetics if we focus on chemical species (e.g. receptor species) instead of compartments. Note, however, that this procedure to obtain MRT in terms of the parameters k_i implies having an analytical (exact) solution of the system, and then, solving some integrals. This is a limitation to extend this idea to a general framework since there are no methods that allow to compute analytical solutions for nonlinear systems, leaving aside the difficulties of evaluating the integrals involved in (8).

From the above paragraphs, we have shown that various approaches addressing the concept of RT have been proposed in the literature, although there is no apparent connection among them: while expression (7) is a detailed description of RT for a specific system, expression (9) provides a general procedure but difficult to compute. On the other hand, expression (7) is often used in the literature without including a proof. It would therefore be desirable to have a rigorous and easy-to-implement general procedure to compute RT. In this paper, we provide a mathematical framework for defining and quantifying RT that can be applied to a general class of biochemical interactions while minimizing computational requirements. In particular, we show its agreement with the RT definitions reviewed in this introduction [1,5,6,7]. Furthermore, we revisit how Eq. (7) and others derived from it were obtained in the literature and, afterwards, take them as a reference to capture the mathematical essence of these parameters and propose a comprehensive definition.

The paper is organized as follows. In the Methods section, we present the necessary mathematical concepts and terminology (namely, linearization around equilibria, dominant eigenvalues and slow manifolds) and we propose the general procedure to compute the residence time. In the Results section, we successfully apply it to compute the drug-target residence time for a selection of pharmacological models, including the binary ligand-receptor complex, the conformational induction model, the two-state receptor model with no interconvertible states, several protein oligomerization models, the allosteric ternary complex and rebinding; we end the results by computing the residence time for other situations beyond drug-target residence time such as the lifetime of active complexes or relaxation times; the mathematical technicalities of the Results section are provided in Appendix D. In the Discussion

section, we compare the proposed method with the above-mentioned approaches (developed in the appendices A, B and C) and we also relate k_{off} to both the catalytic constant k_{cat} used in enzymology and the concept of half-life.

2. Materials and methods

We propose a general procedure for the quantification of RT based on the computation of a relevant parameter associated to the linearization of the system around an equilibrium point. We will see that this parameter is well-defined under generic conditions.

2.1. Definition of residence time

We will assume to have a mathematical model of the biochemical reaction consisting of an ordinary differential equation (ODE) system derived from the Law of Mass Action, which states that the variation over time of the concentration of a compound is proportional to the concentration of the reactants involved in the process through the microscopic rate constants. Let us denote the system as

$$\frac{dx}{dt} = X(x). \tag{10}$$

In general, we assume to have n species, so that $x = (x_1, \ldots, x_n)$ and the variable x is the vector of the concentrations of all chemical species. For the case of ligand binding followed by receptor activation, see Eq. (6), the system is written as

$$\begin{cases} \dfrac{dx_1}{dt} = -(k_{-1} + k_2)x_1 + k_{-2}x_2 + k_1\left([L]_{tot} - x_1 - x_2\right)\left([R]_{tot} - x_1 - x_2\right), \\ \dfrac{dx_2}{dt} = k_2 x_1 - k_{-2}x_2, \end{cases} \tag{11}$$

where x_1 and x_2 represent [LR] and [LR*], respectively. The concentrations of the free receptor and the free ligand have been substituted, respectively, by $[R] = [R]_{tot} - x_1 - x_2$ and $[L] = [L]_{tot} - x_1 - x_2$, where $[R]_{tot}$ and $[L]_{tot}$ are the total concentrations of the two species. In the notation of Eq. (10), $x = (x_1, x_2)$ and the vector field X has two components, corresponding to the two right-hand sides of the equations in system (11).

Note that system (10) can have different equilibria, that is, values x_{eq} of the concentrations such that $X(x_{eq}) = 0$. In biological processes, the observable equilibria are the *attractors*, see [8] for a definition, that is, the equilibrium points x_{eq} such that there exists an open neighbourhood U for which all trajectories with initial conditions in U tend to x_{eq} as time goes to infinity. In the context of models derived from the Law of Mass Action it is often the case that there is a single attractor. For the sake of simplicity, then, we will focus on systems with a unique attractor, but all the methodology could be applied in the presence of multiple attractors.

It is known from the theory of dynamical systems —more precisely, the Hartman-Grobman Theorem, see [9,10]— that in generic situations the system can be linearized around an attractor. This means that, near x_{eq}, the solutions of system (10) are *homeomorphic* (i.e. have the same qualitative properties) to the solutions of a linear system

$$\frac{dx}{dt} = Ax, \tag{12}$$

where A is an n x n real matrix. In fact, A is the so-called *Jacobian matrix* of X evaluated at x_{eq}. The eigenvalues of A play a fundamental role here (a value λ such that A v= λv for a particular vector v is called an *eigenvalue* of A, while the vector v is known as an *eigenvector* associated to the eigenvalue λ). The eigenvalues can also be defined as the roots of the characteristic polynomial associated to the matrix A, see [8].

From basic linear algebra, if x_{eq} is an attractor, the generic situation is that A has all eigenvalues with negative real part and that the solutions of system (12) can be written as

$$x(t) = c_1 v_1 e^{\lambda_1 t} + \cdots + c_n v_n e^{\lambda_n t}, \tag{13}$$

where the v_i are the eigenvectors of the system, λ_i are their corresponding eigenvalues, and c_i are constants depending on the initial conditions. Note that, in principle, all factors can be either real or complex numbers. Let us assume, without loss of generality, that $Re(\lambda_n) \leq Re(\lambda_{n-1}) \leq \ldots \leq Re(\lambda_2) \leq Re(\lambda_1) < 0$, where $Re(\lambda)$ stands for the real part of λ. Following this notation, another generic situation is that one of the two following conditions happens:

(H1) λ_1 is real and $Re(\lambda_n) \leq Re(\lambda_{n-1}) \leq \ldots \leq Re(\lambda_2) < \lambda_1 < 0$.

(H2) λ_1 and λ_2 form a pair of complex conjugate numbers, that is $\lambda_{1,2} = \alpha \pm \beta i$, with $i^2 = -1$, and $Re(\lambda_n) \leq Re(\lambda_{n-1}) \leq \ldots \leq Re(\lambda_3) < \alpha < 0$.

The case (H1) corresponds to an overdamped oscillation whereas the case (H2) to a damped oscillation, see Fig. 1.

Under these conditions, we define k_{off} without ambiguity as

$$k_{off} = |Re(\lambda_1)|. \tag{14}$$

Consequently, from (5), we have that the residence time is defined as

$$\tau = \frac{1}{|Re(\lambda_1)|}. \tag{15}$$

Since the most common situation in binding kinetics is (H1) and our results can be easily extended to the case (H2), in order to ease the exposition, we will assume that (H1) holds. In this case,

$$k_{off} = |\lambda_1| \text{ and } \tau = \frac{1}{|\lambda_1|}. \tag{16}$$

We will refer to λ_1 as the *smallest-modulus eigenvalue*. Fig. 2 shows a two-dimensional representation of the generic situation we are considering. The blue line represents the line whose direction vector is v_1. In the terminology of dynamical systems, this line is called the *slow manifold* of the linearized system (12); moreover, the Hartman-Grobman Theorem states that all solutions $(x_1(t), \ldots, x_n(t))$ of system (10) that tend to x_{eq} (black trajectories in Fig. 2) will do so tangentially to the blue line. This fact is crucial for our purposes: it claims that the characteristic time of all orbits will be governed by the term $e^{\lambda_1 t}$, see Eq. (13).

For readers less familiar with the concepts of eigenvalues and eigenvectors, we explain that in the context of this article (hypothesis H1), the existence of an eigenvector whose eigenvalue is at least one order of magnitude smaller in modulus than the others implies the presence of a preferred direction of approach to the equilibrium point in the multi-dimensional space where the system's dynamics evolve —specifically, the space of species concentrations. Practically, this means that the time required to reach equilibrium, which is directly related to the residence time, is primarily determined by a single direction. In essence, this represents a form of dimensionality reduction, governed by principles similar to those of principal component analysis [11]. This reduction allows us to characterize the temporal dynamics near equilibrium with a single parameter, k_{off}.

This interpretation agrees with the remark made by Johnson [5] that any reaction in a sequence of reactions that is much faster than the one included in the preceding step will not be observed as a distinct reaction but will occur at the rate of the preceding step. Every step in a sequence of reactions will provide an exponential term to the general solution, but it will decay rapidly because of its fast rate. The absolute value of an eigenvalue describes how fast the step rate is: the higher the absolute value, the faster the rate is, and therefore, the faster it decays and the more imperceptible it becomes.

This idea is also supported by more recent literature [12,13], where the exponential with smallest-modulus eigenvalue (i.e. the slowest component of the system) is said to be the one that generates k_{obs} and k_{off} from experimental measurements. To illustrate this assessment, in Fig. 3 we show several solutions of system (11) which are, indeed, linear

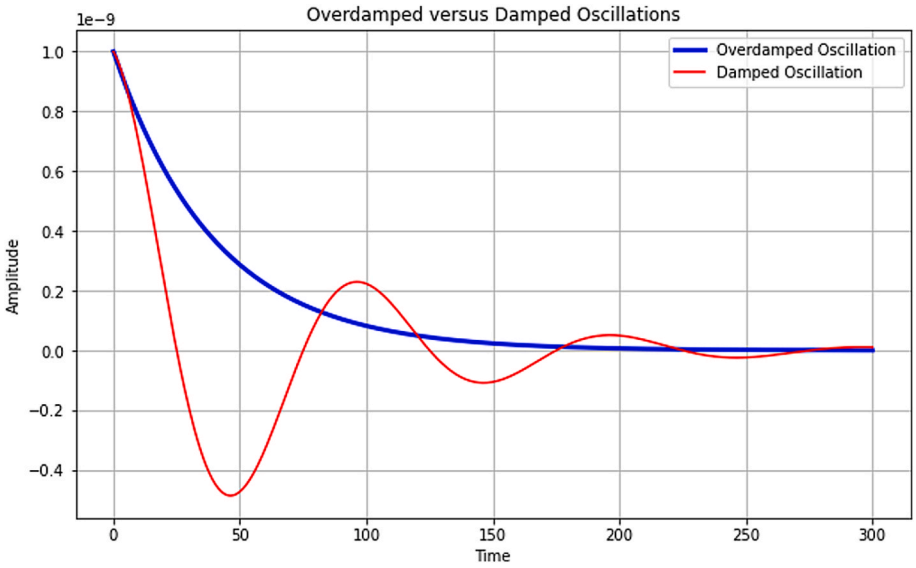

Fig. 1. Overdamped versus damped oscillations (generic example). Our study focuses on overdamped oscillations, but it can be easily extendable to damped oscillations.

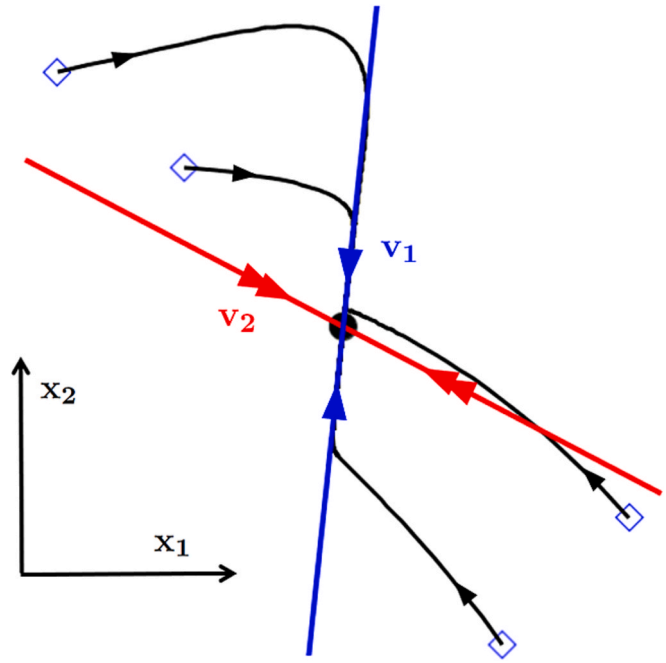

Fig. 2. Schematic representation of the trajectories of a generic nonlinear 2D-system in a neighbourhood of an attractor point (equilibrium point) with two negative eigenvalues associated, say λ_1 and λ_2 such that $\lambda_2 < \lambda_1 < 0$. Axes represent the concentrations of two species. The blue line is the direction corresponding to the smallest-modulus eigenvalue (λ_1), that is, the direction of v_1, thus indicating the linear slow manifold associated to the equilibrium point. The red line is the direction corresponding to v_2, the eigenvector of eigenvalue λ_2; double arrow identifies it as the fast direction. Black curves represent orbits of the nonlinear system starting at four different initial conditions (marked with squared symbols). Note that these orbits tend to the equilibrium point (black dot) as time evolves and, importantly, tangent to the direction of v_1.

combinations of two exponentials, as expressed in Eq. (13). In each panel, a value of $K_R = k_{-2}/k_2$ is fixed ($K_R = 0.02$ in panel A and $K_R = 0.2$ in panel B), and three solutions corresponding to three values of k_2 are displayed. For reasons explained in Section 2.2, we consider $k_1 = 0$. Notice that, although being constructed as a combination of exponentials, every curve in Fig. 3 could be analyzed as a single decaying exponential.

2.2. Subsystem of interest and effective computation of k_{off}

In any chemical process it may happen that only a part of it (the *subsystem of interest*) determines the RT. Thus, we need to define which chemical species are of interest, and then omit their global formation processes. For instance, in the example of system (11), corresponding to chemical process (6), since we want to obtain the residence time of ligand L in receptor R, the chemical species of interest are LR and LR*, with x_1 and x_2 being the corresponding concentrations. In the proposed procedure, only the equations of the chemical species of interest are considered, and the rest are discarded. Because system (11) consists only of the two ODEs corresponding to these variables, it is not necessary to discard any equation. However, there are processes that do not influence the RT, like the association processes of the ligand: because RT measures the duration of the ligand-receptor complexed species, the ligand association process, governed by k_1, should be neglected. This decision would not apply to forward and backward rate constants k_2 and k_{-2} because they involve a conformational change once the LR complex is formed. Paraphrasing to [1] by using the human analogy of RT as that of one's residence time at a hotel, the charges for a hotel stay are not influenced by how long it takes one to arrive at the hotel (k_1), but the period of time between check in (analogous to the bound state) and check out (analogous to dissociation). Also, because the guest may change the room during their stay and this may have an extra cost, k_2 and k_{-2} need to be included. The translation of these ideas into a mathematical expression would be setting $k_1 = 0$. Moreover, we can see that the effect of this condition is equivalent to making $[L] = [L]_{tot} - x_1 - x_2 = 0$ in system (11). The latter condition can be envisaged as a fast ligand elimination process in an experimental situation. In consequence, either by making $k_1 = 0$ or $[L] = 0$, the ligand association process is obviated and the last term in dx_1/dt in system (11) disappears, leading to the following subsystem:

$$\begin{cases} \dfrac{dx_1}{dt} = -(k_{-1} + k_2)x_1 + k_{-2}x_2, \\ \dfrac{dx_2}{dt} = k_2 x_1 - k_{-2}x_2. \end{cases} \tag{17}$$

In the new ODE system, both x_1 and x_2 concentrations will present a

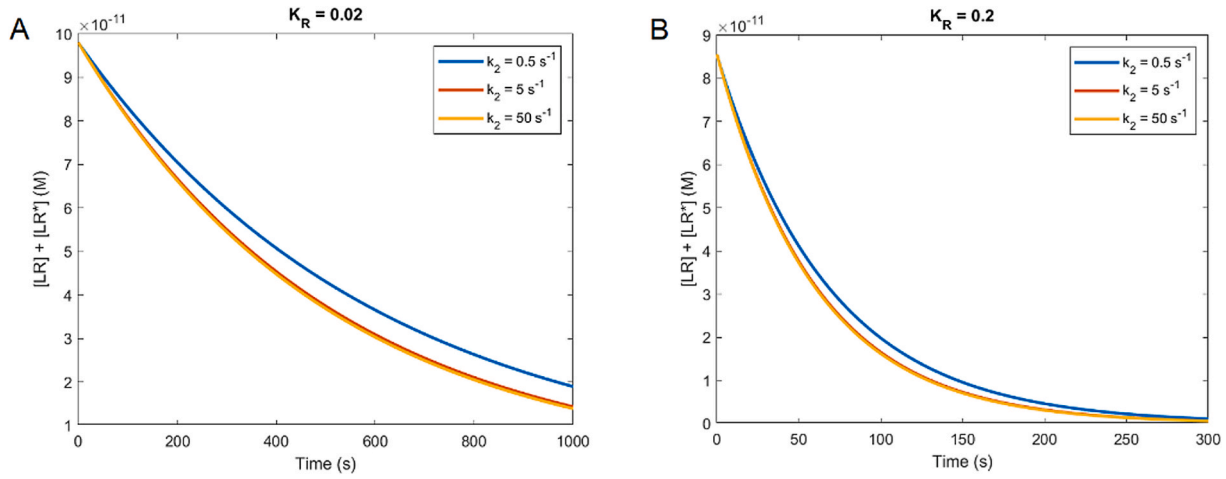

Fig. 3. Representation of the ligand-receptor complex decay over time for the chemical Eq. in (6) when there is no association of the ligand ($k_1 = 0$), see system (11). The analytical solution for each chemical species is a linear combination of exponential functions that have the eigenvalues of the system as the coefficients of their exponents, as in equation (13). The initial condition in all the provided examples is the equilibrium point of the same system when association is considered ($k_1 \neq 0$), with $L_{tot} = 10^{-8}$ M and $R_{tot} = 10^{-10}$ M. The values for the ligand binding process, $k_1 = 10^7$ M^{-1} s^{-1} and $k_{-1} = 0.1$ s^{-1}, were taken from [3]. Two values for the dissociation equilibrium constant $K_R = k_{-2}/k_2$ were chosen for the respective panels, A) $K_R = 0.02$ and B) $K_R = 0.2$. We selected in each case the test values of 0.5, 5 and 50 s^{-1} for k_2, while k_{-2} can be obtained as $k_2 K_R$.

decay time different from that of the full system (11). RT is strongly related to this decay because, in absence of association processes, the driving force of the system is the global dissociation rate constant (k_{off}).

The formalism included in this section is also a mathematical translation of typical experimental procedures. First, ligands and receptors are incubated until ligand-receptor complexes are at equilibrium. Then, there are two procedures which are equivalent to making $k_1 = 0$: 1) washout of the free ligand or 2) addition of a second ligand in a high concentration, resulting in a competition assay favoring the binding of the ligand in high excess [2,14,15,16,17], the high concentration of the second ligand prevents the dissociated first ligand from binding again. So, from the perspective of the ligand of interest (the first ligand), we only see the decay of the corresponding ligand-receptor complex [2].

We will explain next how to apply the procedure to find the smallest-modulus eigenvalue λ_1 for two-dimensional systems having a generic expression

$$\begin{cases} \dfrac{dx_1}{dt} = F(x_1, x_2) \\ \dfrac{dx_2}{dt} = G(x_1, x_2) \end{cases} \tag{18}$$

In fact, in this article, we will deal mainly with two-dimensional subsystems of interest, but the procedure is easily extended to higher-dimensional cases (e.g., where there are more than two species involved in determining the RT).

To obtain the eigenvalues of the system, one must compute the Jacobian matrix

$$J = \begin{pmatrix} \dfrac{\partial F}{\partial x_1} & \dfrac{\partial F}{\partial x_2} \\ \dfrac{\partial G}{\partial x_1} & \dfrac{\partial G}{\partial x_2} \end{pmatrix}, \tag{19}$$

where $\frac{\partial}{\partial x_1}$ and $\frac{\partial}{\partial x_2}$ stand for the partial derivatives of the functions F and G with respect to the variables x_1 and x_2, respectively. Note that for a system with n variables (species) we get an *n x n* square matrix.

The eigenvalues are, by definition, the roots (zeros) of the so-called *characteristic polynomial* $P(\lambda) = \det(J - \lambda Id)$, where Id is the identity matrix. Therefore, they are obtained by solving

$$det(J - \lambda Id) = 0 \tag{20}$$

For two-dimensional systems, $P(\lambda)$ is a polynomial of degree two and its roots, $\lambda_{1,2}$, can be written in terms of the *trace* (the sum of entries in the diagonal of J) and the *determinant* of the Jacobian matrix:

$$\lambda_m = \frac{tr(J) - (-1)^m \sqrt{tr(J)^2 - 4det(J)}}{2}, m \in \{1, 2\}. \tag{21}$$

In Eq. (21), whenever $tr(J)^2 - 4det(J) > 0$, we are under hypothesis (H1). If the expression $tr(J)^2 - 4 det(J)$ were negative, we would be under hypothesis (H2). The case $tr(J)^2 = 4det(J)$ is not included neither in (H1) nor in (H2) and it would require a deeper study. However, as it is aforesaid, (H1) is the most common situation in binding kinetics.

When the trace is negative (as it is the case with all the examples in Section 3), for two-dimensional systems, the formula for k_{off} in terms of the trace and the determinant of J according to definition (14) is:

$$k_{off} = \frac{-tr(J) - \sqrt{tr(J)^2 - 4det(J)}}{2}. \tag{22}$$

Note that, for the purpose of this study, it is not necessary to compute the complete solution of the system, that is, $x_1(t)$ and $x_2(t)$, because the eigenvalues are sufficient to obtain the RT according to our proposal.

2.3. Curve fitting

To estimate the relevant parameters of the different exponential decays considered, a standard nonlinear least-squares curve fitting approach was used. Parameter fitting was primarily conducted using the *curve_fit* function from Python 3.11.10. By default, this function uses the Levenberg-Marquardt (*lm*) algorithm, which is well-suited for problems with a sufficient number of data points and assumes unconstrained optimization. However, in cases with fewer experimental points or when parameter bounds were necessary, the *Dogbox* algorithm was used instead, as it handles bound constraints more effectively (see Section 3.5 for details). To validate the robustness and consistency of the fitting procedure, results obtained from Python were compared to those generated using GraphPad Prism 10.4.1, a widely adopted software in pharmacological data analysis. Across all datasets, the estimated parameters from both methods showed good agreement.

3. Results

A number of pharmacological cases have been selected to show the applicability of the procedure. First, to illustrate and validate the proposed formalism, we start with the simplest case, the binary ligand-receptor complex, and continue with the conformational induction model, widely present in the literature. Then, we progressively increase mechanistic complexity.

3.1. The binary ligand-receptor complex

In the case of the binary ligand-receptor complex, see Eq. (1), there is no distinction between conformations or states of the receptor; there is only a single ligand-receptor species, LR, which, in our terminology, is the chemical species of interest. Therefore, if ligand association is omitted ($k_1 = 0$ in Eq. (2)), the resulting differential equation is:

$$\frac{d[LR]}{dt} = -k_{-1}[LR]. \tag{23}$$

Note that Eq. (23) is the differential equation for a simple exponential decay. The only eigenvalue of this system is $\lambda_1 = -k_{-1}$, and $k_{off} = k_{-1}$ in accordance with definition (14). Moreover, the RT is the inverse of k_{off}: $\tau = 1/k_{-1}$. As it is aforesaid, this is an obvious result that is included herein only to show the consistency of the proposal.

3.2. The conformational induction model

Eq. (6) shows the conformational induction model, also known as *induced-fit model*, in which a ligand L binds a receptor R to form the binary LR complex and then induces a conformational change in the receptor complex to generate LR*. LR is assumed to be an inactive state of the receptor while LR* is the active state, i.e. the state that must be formed to trigger signal transmission and pharmacological response.

Unlike the case in Section 3.1, there are now two chemical species of interest, LR and LR*, giving rise to the two-dimensional ODE system (17), the so-called *system of interest*, to define RT. Following the computations developed in Appendix D.1, we obtain

$$k_{off} = |\lambda_1| = \frac{(k_{-1} + k_{-2} + k_2) - \sqrt{(k_{-1} + k_{-2} + k_2)^2 - 4k_{-1}k_{-2}}}{2}. \tag{24}$$

From Eq. (24), we get the RT (τ):

$$\tau = \frac{1}{k_{off}} = \frac{2}{(k_{-1} + k_{-2} + k_2) - \sqrt{(k_{-1} + k_{-2} + k_2)^2 - 4k_{-1}k_{-2}}}. \tag{25}$$

It is worth noting that the expression of k_{off} in Eq. (7), which is typically found in the literature, is equal to –det(J)/tr(J), and this result can be obtained through a Taylor series approximation of Eq. (24) (see Johnson's approach to k_{off} in Section 4.1 and Appendix A).

3.3. The two-state receptor model with no interconvertible states

Guo et al. [16] extended the competition association assay mathematical model [18] to a two-state receptor model where the states R_1 and R_2 of a receptor are not interconvertible and a ligand L can bind to both of them. Schematically, we have:

$$L + R_1 \underset{k_{-1}}{\overset{k_1}{\rightleftarrows}} LR_1 \quad L + R_2 \underset{k_{-2}}{\overset{k_2}{\rightleftarrows}} LR_2 \tag{26}$$

Note that this system is mathematically equivalent to having two different receptors. It is worth stating that in the work of Guo et al. [16] the concept of eigenvalue is used to solve the system and study its stability. However, RT, although briefly mentioned in the introduction, was not calculated. Thus, our purpose is to apply our methodology to the model to obtain RT through both receptor complexes. Accordingly, we choose LR_1 and LR_2 as the chemical species of interest. Following our procedure, the association processes of the ligand are omitted, so that Eq. (26) simplifies to

$$L + R_1 \underset{k_{-1}}{\leftarrow} LR_1 \quad L + R_2 \underset{k_{-2}}{\leftarrow} LR_2 \tag{27}$$

and the subsystem of interest is

$$\begin{cases} \dfrac{d[LR_1]}{dt} = -k_{-1}[LR_1], \\ \dfrac{d[LR_2]}{dt} = -k_{-2}[LR_2]. \end{cases} \tag{28}$$

It can be seen that system (28) consists of two separate exponential decays, governed by k_{-1} and k_{-2}. They are analogous to the case in Eq. (23). Hence, depending on which rate constant is smaller, RT will be $1/k_{-1}$ or $1/k_{-2}$. In the article by Guo et al. [16], the values of the rate constants are conveniently provided. For example, for the ligand ^{3}H-NECA, $k_{-1} = 0.046$ min^{-1} and k_{-2} is 0.0076 min^{-1}. Because k_{-2} is the smallest value, we propose that RT for ^{3}H-NECA is $\tau = 1/0.0076$ min^{-1} = 131.58 min. For the ligand CPA, $k_{-1} = 0.025$ min^{-1} and k_{-2} is 0.0095 min^{-1}; in this case, $\tau = 1/0.0095$ min^{-1} = 105.26 min.

To illustrate the time course of the exponential decay in this system, we studied the decay of ^{3}H-NECA – receptor complexes (Fig. 4). We were provided with data from 2 of the total 5 independent experiments performed to obtain Fig. 2B from [16].

In Fig. 4, a clear distinction can be observed between the curves fitted using monophasic and biphasic decay models. When the difference between the two is minimal, the dominant term of the biphasic decay should closely resemble the monophasic decay (resulting in similar half-lives). However, this is clearly not the case here. Although monophasic fitting is commonly applied in this type of experiment, it would be inappropriate in this instance. The underlying mechanism (as described in Eq. (27) and Eq. (28) involves two distinct processes governed by the rate constants k_{-1} and k_{-2}, which correspond to the absolute values of the system's eigenvalues. Each process provides an exponential term to the analytical solution, explaining why the biphasic model provides a better fit to the data points. The fitting results are summarized in Table 1. For the biphasic model, the estimated eigenvalues are 0.033 and 0.007, corresponding to k_{-1} and k_{-2}, respectively. These values differ slightly from those reported in the original publication, as only 2 of the 5 available experiments were used in our analysis. Since 0.007 is the slower rate constant, it defines the system's dominant timescale, giving $\tau = 1/0.007 = 142.8$ min. These findings are further discussed in Section 4.3.

3.4. Receptor oligomerization models

Protein oligomerization is an evolutionary mechanism for regulating protein function through protein–protein interactions. Homodimers and higher-order oligomers mediate and regulate gene expression, activity of enzymes, ion channels, receptors, and cell–cell adhesion processes [19]. A recent review, focused on the modulation of protein oligomerization based on its mechanism of action, including both *in vitro* and *in vivo* approaches, and several experimental techniques, showed that a significant fraction of cellular proteins, in both prokaryotic and eukaryotic systems, have oligomeric properties [20]. Interestingly, and by using AlphaFold2 artificial intelligence tool to predict homo-oligomeric assemblies across four proteomes, it was found that approximately 45 % of an archaeal proteome and a bacterial proteome and 20 % of two eukaryotic proteomes form homomers [21]. Protein oligomerization is also present in GPCRs, for which, depending on the class/family, there exist obligate or transient homodimers. GPCR oligomerization has been extensively analyzed by mathematical modeling through equilibrium

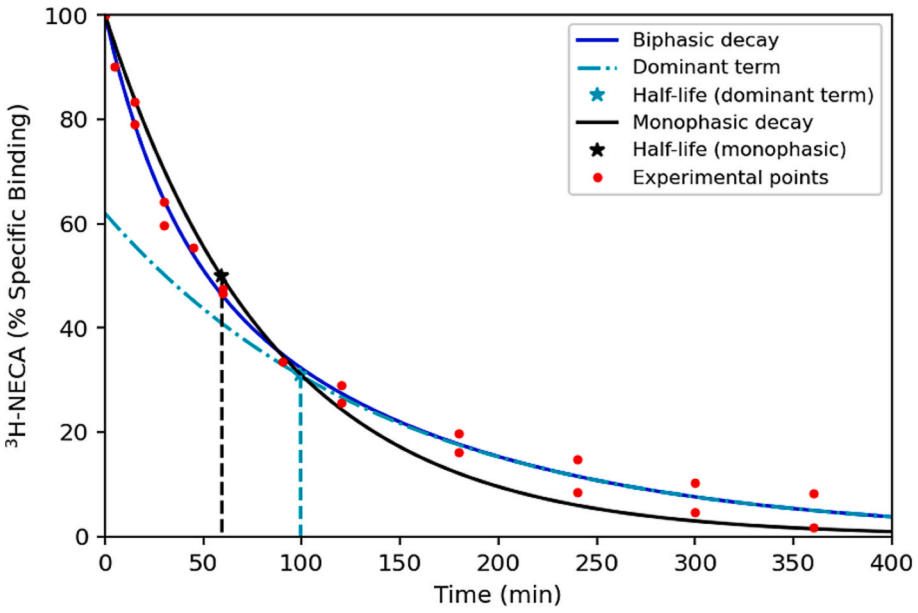

Fig. 4. Fitting of the experimental data from Fig. 2B of [16] either to a monophasic ($y = 100e^{-\lambda t}$) or biphasic ($y = Ce^{-\lambda_1 t} + (100 - C)e^{-\lambda_2 t}$) exponential decay. The half-lives of both the monophasic decay and the dominant term of the biphasic decay are shown to be compared. Fitting was performed by using the data of 2 out of 5 total independent experiments.

Table 1
Parameter values obtained from the fitting of the experimental data from Fig. 2B of [16] either to a monophasic ($y = 100e^{-\lambda t}$) or biphasic ($y = Ce^{-\lambda_1 t} + (100 - C)e^{-\lambda_2 t}$) exponential decay. Fitting was performed by using the data of 2 of the total 5 independent experiments. RT of ^{3}H-NECA was computed for each form of decay.

Function	Parameters	RT (min)	R^2
Biphasic decay	$C = 62 \pm 11$ $\lambda_1 = 0.007 \pm 0.001$ (min^{-1}) $\lambda_2 = 0.033 \pm 0.009$ (min^{-1})	142.8 ($1/\lambda_1$)	0.9934
Monophasic decay	$\lambda = 0.0117 \pm 0.0006$ (min^{-1})	85.5 ($1/\lambda$)	0.97323

constants (see [22] for review) or from a kinetic perspective [3,23,24]. However, despite its pharmacological relevance, the quantification of residence time has not yet been addressed. We will discuss this topic, considering the cases of homodimeric, homotetrameric and heterodimeric receptors.

3.4.1. The homodimeric receptor model

The binding processes of a ligand to a homodimeric receptor [24,25] follow the scheme

$$2L + RR \underset{k_{-1}}{\overset{2k_1}{\rightleftarrows}} L + LRR \underset{2k_{-2}}{\overset{k_2}{\rightleftarrows}} LRRL \tag{29}$$

The factors multiplying k_1 and k_{-2} have been included because, for the former rate constant, the singly-occupied receptor LRR can be formed by ligand binding to any of the two sites of the receptor while, for the latter, the doubly-occupied receptor LRRL can dissociate from any of the two sites. In this way, the rate constants in Eq. (29) are treated as microscopic rate constants (see [26]). To solve this case and following our formalism, two cases of interest can be considered: the RT of the occupied receptor (either doubly or singly-occupied) and the RT of the doubly-occupied receptor.

3.4.1.1. The doubly-occupied homodimer model. If the functional response is elicited only when the homodimeric receptor is fully occupied, then LRRL will be the only chemical species of interest. In this case, the decay of this receptor species (defined by the rate constant $2\,k_{-2}$) will define the RT. The situation is analogous to the binding of a single ligand to a receptor, which has been described in Eq. (23). Thus, the corresponding ODE system is

$$\frac{d[LRRL]}{dt} = -2k_{-2}[LRRL], \tag{30}$$

and the RT is $\tau = 1/(2\,k_{-2})$.

Note that the formalism for receptor homodimerization, and higher-order oligomers, in general, can be directly translated to the case of ion channels with two or more binding sites, respectively [26].

3.4.1.2. The doubly and singly-occupied homodimer model. If our focus is on both the doubly and the singly-occupied homodimers, then the subsystem scheme becomes

$$2L + RR \underset{k_{-1}}{\leftarrow} L + LRR \underset{2k_{-2}}{\leftarrow} LRRL \tag{31}$$

which leads to the system

$$\begin{cases} \dfrac{d[LRRL]}{dt} = -2k_{-2}[LRRL], \\ \dfrac{d[LRR]}{dt} = 2k_{-2}[LRRL] - k_{-1}[LRR]. \end{cases} \tag{32}$$

Depending on which one is smaller, the RT of ligand L will be $1/(2\,k_{-2})$ or $1/k_{-1}$ (see Appendix D.2). Notice that this is a similar situation to the one described previously in Section 3.3.

3.4.2. The homotetrameric receptor model

GPCRs can oligomerize in higher-order arrangements than homodimers. In particular, homotetramers can be formed (see, for example, references to the M_2 muscarinic receptor in [27]). Of note, a mathematical model for the interconversion between two homodimers and a tetramer was proposed and their relative stoichiometry and ligand binding analyzed in terms of equilibrium constants [28]. We take here the homotetramer system and replace equilibrium by rate constants to compute the RT.

$$4L+R_4 \underset{k_{-1}}{\overset{4k_1}{\rightleftarrows}} 3L+LR_4 \underset{2k_{-2}}{\overset{3k_2}{\rightleftarrows}} 2L+L_2R_4 \underset{3k_{-3}}{\overset{2k_3}{\rightleftarrows}} L+L_3R_4 \underset{4k_{-4}}{\overset{k_4}{\rightleftarrows}} L_4R_4 \quad (33)$$

$$4L+R_4 \underset{k_{-1}}{\leftarrow} 3L+LR_4 \underset{2k_{-2}}{\leftarrow} 2L+L_2R_4 \underset{3k_{-3}}{\leftarrow} L+L_3R_4 \underset{4k_{-4}}{\leftarrow} L_4R_4 \quad (34)$$

As it can be seen in Eq. (33), there are four ligand-receptor binding processes since there are four binding sites for a homotetramer. Eq. (34) describes the system when all the association processes of the ligand are omitted. In the same way as in Eq. (29), the factors multiplying the rate constants were included to treat them as microscopic rate constants. As in the homodimer case, we can again consider different situations. Namely, if the only chemical species of interest is the fully-occupied homotetramer, L_4R_4, then its concentration will follow a simple exponential decay ruled by $-4k_{-4}$ (in an analogous form to Eq. (30)) and RT would be $1/(4\ k_{-4})$; but, if the chemical species of interest are all the ligand-bound homotetramers, whether fully or partially occupied, then the system is more complex (see the equations of the systems and the corresponding computations in Appendix D.3).

The RT of ligand L will be either $1/(4\ k_{-4})$, or $1/(3\ k_{-3})$, or $1/(2\ k_{-2})$ or $1/k_{-1}$, depending on which one is the smallest in absolute value. As shown in Appendix D.3, the results can be easily extended to homomers with n protomers, for which $\tau = \max_{m=1,\cdots,n}\left\{\frac{1}{mk_{-m}}\right\}$.

3.4.3. The heterodimeric receptor model

Receptors can oligomerize not only forming homo-oligomers but also hetero-oligomers [29]. A heterodimer receptor model in a binding kinetics context was recently proposed [3], see Fig. 5. The solution of the time-dependent concentrations of the chemical species was provided in [23]. Quantification of residence time will complement and reinforce the binding kinetics subject in the field.

Heterodimeric receptors can yield pharmacological responses that differ from those produced by their partners when acting as monomers [30,31]. Moreover, if we accept that a heterodimeric receptor provides the conceptual framework for drug combination therapy [23], then we will consider the receptor species of interest as that with both ligands bound, i.e. AR_1R_2B. Thus, residence time refers to the case of both ligands bound to the receptor. If, following our rationale, AR_1R_2B formation processes are omitted (i.e., k_3 and k_4 are not considered), the scheme of the subsystem of interest is

$$AR_1R_2+B \underset{k_{-3}}{\leftarrow} AR_1R_2B \underset{k_{-4}}{\rightarrow} A+R_1R_2B \quad (35)$$

and the corresponding ODE subsystem is one-dimensional:

$$\frac{d[AR_1R_2B]}{dt} = -(k_{-3}+k_{-4})[AR_1R_2B]. \quad (36)$$

Therefore, there is a single eigenvalue, $\lambda_1 = -(k_{-3}+k_{-4})$, which leads to the following expressions for k_{off} and RT (τ):

$$k_{off} = |\lambda_1| = k_{-3}+k_{-4},\ \tau = \frac{1}{k_{off}} = \frac{1}{k_{-3}+k_{-4}}. \quad (37)$$

3.5. The allosteric ternary complex model

Allosteric modulation seems to be a general property of living systems and can be considered as a unifying mechanism for receptor function and regulation [32]. Allosteric interactions between ligands can happen not only through protein–protein interactions in receptor oligomers but also through two binding sites (the orthosteric and the allosteric) in a single receptor protein. The simplest model for allosteric interactions in a single receptor is the allosteric ternary complex model depicted in Fig. 6 (see [33,34] for review). Ligand A is considered to bind to the orthosteric site, while ligand B binds the allosteric site acting as a positive (PAM), negative (NAM) or neutral allosteric modulator [3]. Although this situation is clearly different from the heterodimeric receptor from a pharmacological point of view, it is mathematically equivalent: two binding sites, four receptor species and eight rate constants (four forward and four reverse) depicted on a formally analogous chemical scheme. Thus, the ODE systems obtained from both models are the same. However, because the heterodimeric receptor and the allosteric ternary receptor models are pharmacologically different systems, the chemical species of interest for the calculation of residence time are also different.

In the case of the heterodimeric receptor, we consider only the doubly-occupied receptor species to be of interest because of the pharmacological context: two-drug combination therapies are the result of the combined effect of two drugs; then, we considered their joint binding to the receptor as that responsible of the selected effect. However, in the case of analyzing the allosteric modulation of an orthosteric ligand in a monomeric receptor, what is interesting to compare is the RT of ligand A alone with that of ligand A in presence of the allosteric modulator B. From the binding kinetics point of view, it would be expected that if B is a PAM, it would increase the RT of ligand A; while if B is a NAM, the opposite result would be found. Mathematically, a PAM would make k_{-4} smaller than k_{-1} (see Fig. 6a), which means that the dissociation rate of ligand A is slower in presence of B. It can be also said that a PAM makes $\alpha_- < 1$, if cooperativity rate parameters are used (see Fig. 6b). These concepts can be better understood in the context of recent experimental work [35]. In the latter study, a ligand, named *368*, was found that, by allosterically binding to the μ-opioid receptor (MOR), increased the affinity of the MOR antagonist naloxone by decreasing its dissociation rate. This was also consistent with experiments showing an increase in naloxone residence time in the presence of *368*. The discovery of *368* is

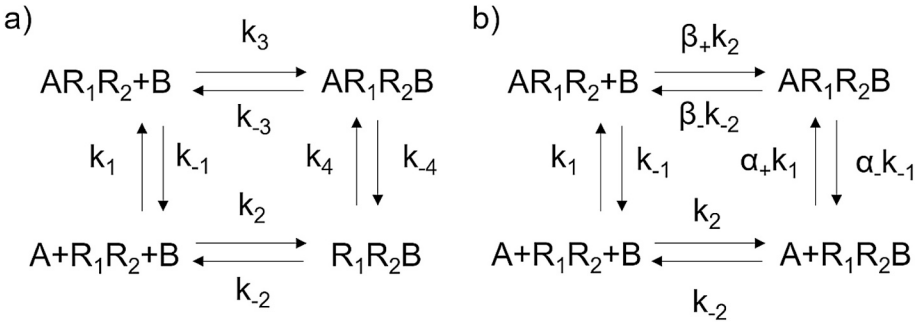

Fig. 5. Diagram of ligand binding to a preformed heterodimeric receptor. Ligand A binds to receptor R_1 protomer and ligand B to R_2. There are four chemical species of the receptor: the empty heterodimer R_1R_2, the singly-occupied heterodimers AR_1R_2 and R_1R_2B, and the doubly-occupied heterodimer AR_1R_2B. **a)** Rate constants numbered from 1 to 4: forward rate constants have positive subscripts, and the backward or reverse ones have negative subscripts. **b)** Introduction of cooperativity rate parameters α_+, α_-, β_+ and β_-: the rate constants with subscripts 3 and 4 (positive and negative) can be expressed in terms of the rate constants with subscripts 1 and 2 (positive and negative) through the cooperativity rate parameters.

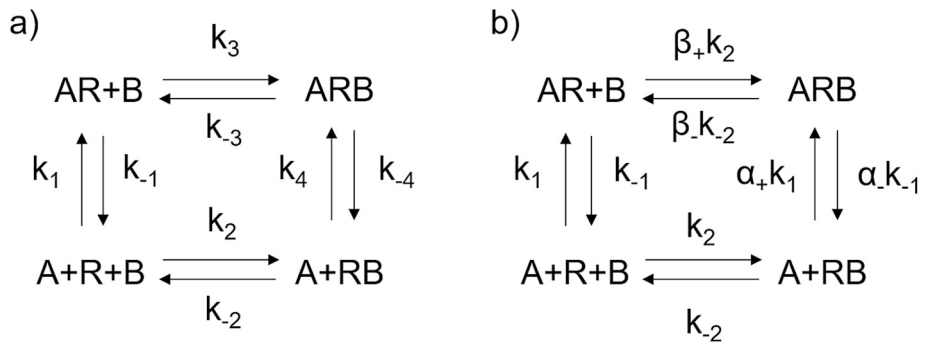

Fig. 6. Diagram of ligand binding to a receptor with two binding sites: one orthosteric and one allosteric. Ligand A binds to the orthosteric binding site and ligand B to the allosteric one. There are four chemical species of the receptor: the empty receptor R, the singly-occupied receptors AR and RB, and the doubly-occupied receptor ARB. Notice the similarity with the diagram for a heterodimeric receptor in Fig. 5. **a)** Rate constants numbered from 1 to 4: forward rate constants have positive subscripts and the backward or reverse ones have negative subscripts. **b)** Introduction of cooperativity rate parameters α_+, α_-, β_+ and β_-: the rate constants with subscripts 3 and 4 (positive and negative) can be expressed in terms of the rate constants with subscripts 1 and 2 (positive and negative) through the cooperativity rate parameters.

of great relevance because naloxone is the most common and effective treatment for opioid overdoses and therefore critical to addressing the current opioid overdose epidemic driven by fentanyl and other highly potent MOR agonists [35]. It is worth noting that we have considered *368* a PAM because it increased the affinity of an orthosteric ligand, while in the original article it was considered a NAM because, being naloxone an antagonist, *368* contributed to the stabilization of the inactive state of MOR and, consequently, to the blocking of agonist binding. The application of our rationale may help to mechanistically quantify the observed increase of naloxone (ligand A) residence time in the presence of *368* (ligand B).

The RT of ligand A in the absence of B is obtained straightforwardly as $1/k_{-1}$ ($k_{off} = k_{-1}$) (see Fig. 6), because it is analogous to the binary ligand-receptor complex described in Section 3.1. If ligand B is present, then the chemical species of interest to obtain the RT of ligand A are AR and ARB, that is, the receptor complexes containing A. The subsystem of interest is then

$$R \underset{k_{-1}}{\leftarrow} AR \underset{k_{-3}}{\overset{k_3}{\rightleftarrows}} ARB \underset{k_{-4}}{\rightarrow} RB \tag{38}$$

In terms of the cooperativity rate parameters, Eq. (38) is written as

$$R \underset{k_{-1}}{\leftarrow} AR \underset{\beta_- k_{-2}}{\overset{\beta_+ k_2}{\rightleftarrows}} ARB \underset{\alpha_- k_{-1}}{\rightarrow} RB \tag{39}$$

The nonlinear ODE system corresponding to the Eq. (38) is studied in Appendix D.4.

For the RT of ligand A to be higher in the presence of B, the k_{off} when A is alone must be higher than the k_{off} obtained for the current model. In the Appendix D.4 it is proven that this fact implies that $k_{-4} < k_{-1}$, which is equivalent to $\alpha_- < 1$. This condition was intuitively expected for PAMs according to Fig. 6, and we can also conclude from this mathematical proof that $\alpha_- > 1$ for NAMs. Moreover, these conclusions would apply to the heterodimeric receptor model due to its mathematical equivalence (see Fig. 5). If one were interested in the RT of ligand A in the heterodimer in the presence of B, with AR_1R_2 and AR_1R_2B as chemical species of interest, then the expression of k_{off} would be the same as (22), with exactly the same trace and determinant shown in (D15). This occurs because, although the allosteric ternary model and the heterodimeric receptor model are clearly different from a pharmacological point of view, they are mathematically equivalent, as both share the same ODE system.

A recent study [36] describes an allosteric model involving the M_4 muscarinic acetylcholine receptor (M_4 mAChR). Using Eq. (38) as a reference, receptor R corresponds to M_4 mAChR, ligand A is ^{3}H-NMS (an orthosteric radioactive ligand) and ligand B is xanomeline, an allosteric modulator that can also bind to the orthosteric site. The study measured the dissociation rate constant (k_{off}) of ^{3}H-NMS under varying concentrations of xanomeline: 0, 10, 30, and 100 μM. These measurements were obtained via a competition binding assay, as outlined in Section 2.2. When ^{3}H-NMS − M_4 mAChR complexes are at equilibrium, a second ligand (atropine in this case) is added at a high concentration resulting in a competition assay that favors atropine binding. An amount of 10 μM of atropine was the minimum necessary concentration to prevent the association of ^{3}H-NMS. However, this assay was also performed by using xanomeline as an excess orthosteric ligand besides as an allosteric ligand. Note that, although xanomeline displays bimodal binding (orthosteric and allosteric), its orthosteric modality is obviated in this case because what is being measured is the RT of ^{3}H-NMS, which is the only labeled ligand. Therefore, the role of xanomeline as an orthosteric ligand, under these circumstances, is just establishing the necessary excess to prevent rebinding of ^{3}H-NMS. An amount of 10 μM of xanomeline was also the minimum necessary concentration to prevent the association of ^{3}H-NMS. The results indicate that, in the situations where a concentration of 10 μM of either atropine or xanomeline is used, a very similar k_{off} is obtained, which corresponds to the k_{off} of ^{3}H-NMS when there is no allosteric modulation, k_{-1}. As the concentration of xanomeline increased, a decrease in k_{off} was observed and, in consequence, the RT of ^{3}H-NMS is extended in presence of higher xanomeline concentrations.

This effect is illustrated in Fig. 7, which compares two dissociation curves: (a) with 10 μM atropine and no xanomeline, and (b) with 100 μM xanomeline. In the latter case, xanomeline not only prevents ^{3}H-NMS rebinding but also exerts a significant allosteric effect. In contrast, atropine at 10 μM serves solely to block rebinding without allosteric modulation, since it is an orthosteric ligand. Thus, the extended residence time seen in the presence of high xanomeline concentrations reflects its allosteric modulation of the ^{3}H-NMS–receptor complex.

In both Fig. 7a and b, the experimental data (accessible online) [36] were fitted to both a monophasic and a biphasic decay, and it can be seen that the curves are coincident. In Fig. 7a, no xanomeline is present, so the k_{-1}-governed decay of ^{3}H-NMS is described. Therefore, from a mechanistic point of view, the correct choice is to use the monophasic decay formula, which gives the eigenvalue $\lambda = 0.0058\ \text{min}^{-1}$ (see Table 2). This value is equal to k_{-1}, which is the only rate constant involved in this process. If we look at the results of the fitting to a biphasic decay, one of the eigenvalues coincides with the one provided by the fit to a monophasic decay, and the other one has a different value, without error. The value of the constant C is 100, which implies the disappearance of the second exponential term in $y = Ce^{-\lambda_1 t} + (100 - C)e^{-\lambda_2 t}$; that is, the fitting algorithm does not distinguish between

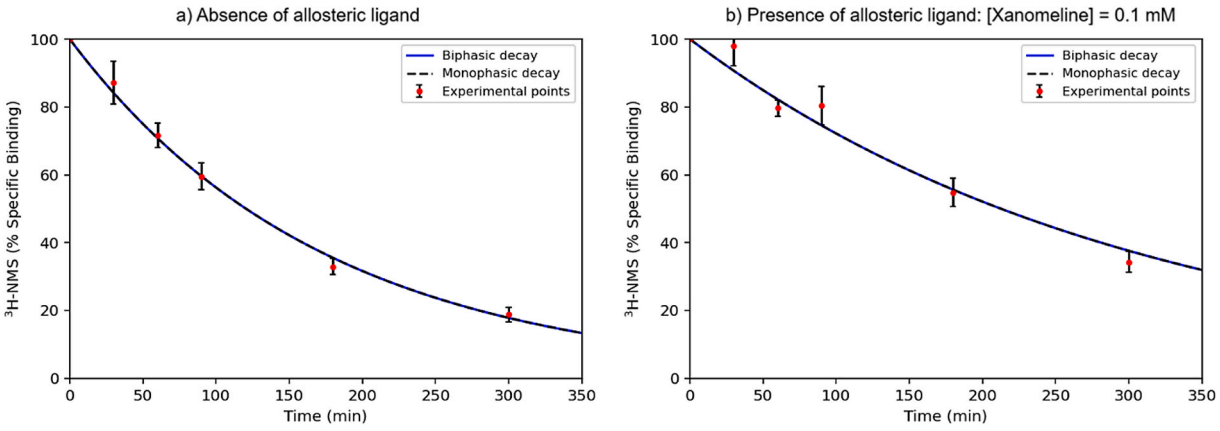

Fig. 7. Fitting of the experimental data from Fig. 3b of [36] either to a monophasic ($y = 100e^{-\lambda t}$) or biphasic ($y = Ce^{-\lambda_1 t} + (100 - C)e^{-\lambda_2 t}$) exponential decay. The decay of ^{3}H-NMS − M_4 mAChR WT complexes over time was considered under two situations: a) in the absence of an allosteric ligand, and b) in the presence of the allosteric ligand xanomeline, with a concentration of 0.1 mM.

Table 2
Parameter values obtained from the fitting of the experimental data from Fig. 3b of [36] either to a monophasic ($y = 100e^{-\lambda t}$) or biphasic ($y = Ce^{-\lambda_1 t} + (100 - C)e^{-\lambda_2 t}$) exponential decay. RT of ^{3}H-NMS in M_4 mAChR WT was computed for each case.

Situation	Function	Parameters	RT (min)	R^2
Absence of allosteric ligand	Biphasic decay	$C = 100 \pm 4$ $\lambda_1 = 0.0058 \pm 0.0004$ (min^{-1}) $\lambda_2 = 0.0683 \pm 0.0$ (min^{-1})	172.4 ($1/\lambda_1$)	0.9966
	Monophasic decay	$\lambda = 0.0058 \pm 0.0002$ (min^{-1})	172.4 ($1/\lambda$)	0.9966
Presence of allosteric ligand xanomeline (0.1 mM)	Biphasic decay	$C = 100 \pm 8$ $\lambda_1 = 0.0033 \pm 0.0006$ (min^{-1}) $\lambda_2 = 0.0442 \pm 0.0$ (min^{-1})	303 ($1/\lambda_1$)	0.9698
	Monophasic decay	$\lambda = 0.0033 \pm 0.0003$ (min^{-1})	303 ($1/\lambda$)	0.9698

two distinct exponential components, instead identifying only a single dominant exponential term. Note that the second eigenvalue can take any arbitrary value (e.g., 0.01, 1, or 1000) since its contribution completely cancels out. The fitting was performed in Python using the *Dogbox* method. However, if GraphPad Prism is used instead, the values for λ_1 and λ_2 will be equal and the errors will be huge. This poor fit to the biphasic exponential decay is mechanistically expected in this case, since it actually describes a monophasic decay of the same type as in Section 3.1.

On the other hand, in the case of Fig. 7b something different happens. Mechanistically, it is expected to have two exponential terms (see Appendix D.4), but if we look at Table 2, we see that something similar to the previous case occurs: the value of the constant C is 100, which cancels the second exponential term. Therefore, one of the eigenvalues (specifically, the one with the highest absolute value) is not detectable. Although this seems inconvenient, it is an ideal example to illustrate what happens when an exponential term is clearly dominant. The exponential term that contains the smallest-modulus eigenvalue, that is, the one that provides the residence time, somehow masks the other exponential term. The second exponential term exists, but its contribution is so small that it is not detectable. In fact, it is so small that the biphasic decay is almost equal to monophasic. Therefore, the result from the monophasic decay can be used without making a significant error. However, it is important to bear in mind that, from a mechanistic point of view, there are two exponential terms: the dominant one and the masked one, and that in these ideal situations, the masked one will not be measurable and can be obviated in practice.

3.6. The rebinding case model

When a ligand dissociates from its receptor, the local concentration of the ligand near the receptor is higher than elsewhere. Because of this fact, it would be more likely for the ligand to bind to the receptor again rather than diffuse away or be eliminated. This phenomenon is called *rebinding*, and when it occurs in a repetitive cycle of rapid rebinding and slow dissociation, it is thought to extend the magnitude of intracellular RT [37]. Note the use of the term intracellular in reference to the RT.

Rebinding can be schematized in the following way:

$$\overset{k_{el}}{\leftarrow} L + R \underset{k_{-1}}{\overset{k_1}{\rightleftarrows}} LR \tag{40}$$

where k_{el} is the elimination or diffusion rate constant for the ligand L.

Note that (40) is built up from (1) by adding an elimination process. Although the definition of the RT is generally accepted as $1/k_{-1}$ for binary ligand-receptor binding processes, there are some proposals in the literature suggesting that k_{on} (k_1 in this particular example), the second order association rate constant, also has an important role in binding kinetics [38,39]. Rebinding processes depend on k_{on} because this is the rate constant that describes the binding of the ligand. To quantify the RT in the context of rebinding we will adapt our methodology and k_{on} will be properly included.

It seems to us that when discussing the role of k_{on} in the RT, the system is approached differently to the more typical ways employed so far in this article: instead of referring to the RT as the time a ligand is expected to remain bound to a receptor, some new terms appear, such as "intracellular RT" or "pharmacokinetics" of the ligand, and usually some references to the elimination constant (k_{el}) of the ligand. It seems that the focus is not on the receptor itself, but also on its environment, or even on the cell; therefore, the RT is now referred to as the time a ligand is expected to remain inside the cell, or in the receptor environment (bound or not) before diffusing.

For this reason, we want to illustrate the rebinding process following Eq. (40) and compare it with Eq. (1). It is clear that in Eq. (1), the ligand RT at the receptor is $1/k_{-1}$; but in Eq. (40), we can distinguish between the ligand RT at the receptor only and the ligand RT in the cell. For the first case, $\tau = 1/k_{-1}$, as in Eq. (1), but if the intracellular RT is desired, then k_{off} is not k_{-1}, but a more complex expression including k_1, k_{-1} and k_{el}. Qualitatively, Eq. (40) is analogous to Eq. (6) when $k_1 = 0$. In Eq. (6), the chemical species of interest are LR and LR* (the RT of the ligand-

receptor complexes), but in this case, they are L and LR (the intracellular RT of the ligand, whether bound or not).

From this point, the methodology for obtaining eigenvalues is applied, see Appendix D.5. In this case, it is not necessary to omit any formation process because the model does not include an influx of ligand L, but only its elimination. It is worth noting that the resulting subsystem of interest is nonlinear in this case. In particular, the Plusquellec and Houin approach for finding the MRT explained in (9) cannot be applied because we cannot find an explicit general expression for the solution. In contrast, it is straightforward to find the smallest-modulus eigenvalue and apply our methodology, which is

$$k_{off} = |\lambda_1| = \frac{k_1[R_{tot}] + k_{el} + k_{-1} - \sqrt{(k_1[R_{tot}] + k_{el} + k_{-1})^2 - 4k_{el}k_{-1}}}{2} \tag{41}$$

This expression for the global dissociation/reverse rate constant includes both association (k_1) and dissociation (k_{-1}) rate constants of the ligand. This idea has already been mentioned in the literature [40], where an "effective reverse coefficient" is defined to better describe this scenario where both k_1 and k_{-1} play a role, instead of using only k_{-1}. This implies that for the case of rebinding, the focus is not put on the receptor itself, but also on its vicinity. So, here, the RT does not refer to the time the ligand spends bound to the receptor before dissociating, but to the time the ligand spends bound to the receptor or being on its surrounding environment before diffusing.

3.7. Extending the concept of drug-target residence time

The procedure presented in this article allows us to extend the concept of RT beyond the limits of ligand-receptor binding. In the context of drug-target RT, the chemical species of interest are all the ligand-target complexes, but we may be interested only in the lifetime of the active receptor species, that is, the lifetime of the receptor species yielding the observed functional response. In this case, we should also consider constitutive receptor activity. Moreover, ligand-receptor binding does not necessarily imply receptor activation, as in the case of antagonists. RT can therefore be redefined as the expected lifetime of the chemical species of interest, whether they are ligand-target complexes or not.

The methodology introduced in the Methods section allows to define also a "residence time" for the above situation. We consider a two-state receptor system (Fig. 8) in which the receptor can be inactive (R) or active (R*). The ligand can bind preferentially to R* (agonist) or R (inverse agonist) or bind to R and R* without preference (neutral antagonist). This situation would correspond to *conformational selection*. Alternatively, the ligand can bind to R forming the LR complex and then induce the activation of the receptor in the complex (LR*), which would correspond to *induction fit*. Although there is a debate about the relative weight of these two trends in real situations [13,41], they probably happen simultaneously, the relative weight depending on the ligand-receptor pair and the cellular environment.

Our aim is to study different situations in terms of the model described in Fig. 8 and to distinguish between different residence times depending on which chemical species of interest are considered or not.

3.7.1. Residence time for ligand-receptor complexes

First, to determine the expression of the RT for ligand-receptor complexes, the diagram in Fig. 8 is simplified to

$$L + R \underset{k_{-2}}{\leftarrow} LR \underset{k_{-4}}{\overset{k_4}{\rightleftarrows}} LR^* \underset{k_{-3}}{\rightarrow} L + R^* \tag{42}$$

The two chemical species of interest are LR and LR*, and the formation processes for these species (governed by k_2 and k_3) are omitted. From the computations in Appendix D.6, we get

$$k_{off} = \frac{k_{-2} + k_{-3} + k_{-4} + k_4 - \sqrt{(k_{-2} + k_{-3} + k_{-4} + k_4)^2 - 4(k_{-2}k_{-4} + k_{-2}k_{-3} + k_{-3}k_4)}}{2}. \tag{43}$$

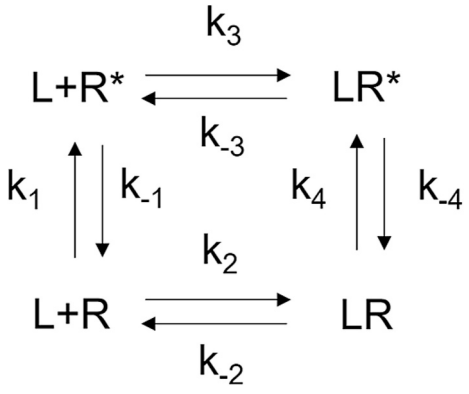

Fig. 8. Two-state receptor model including both conformational selection and induction-fit mechanisms. Induction-fit consists of receptor activation after ligand binding, while conformational selection assumes that the receptor can be active in the absence of the ligand. Therefore, there are four reversible reactions and four chemical species in this system: the inactive receptor (R), the active receptor (R*), the inactive ligand-receptor complex (LR) and the active ligand-receptor complex (LR*). Note that only seven of the eight rate constants are independent since the relationship $\frac{k_{-1}k_{-3}}{k_1k_3} = \frac{k_{-2}k_{-4}}{k_2k_4}$ holds.

3.7.2. Residence time of the active ligand-receptor complex

Another mechanistic condition within the scheme of Fig. 8 would be to consider that the only chemical species of interest is LR*, the only ligand-receptor complex yielding the functional response. After eliminating its formation processes (governed by k_3 and k_4), the scheme is reduced to

$$L + R^* \underset{k_{-3}}{\leftarrow} LR^* \underset{k_{-4}}{\rightarrow} LR \tag{44}$$

whose corresponding ODE is

$$\frac{d[LR^*]}{dt} = -(k_{-3} + k_{-4})[LR^*]. \tag{45}$$

This case is analogous to the one described in Eq. (23), and therefore the RT of the ligand bound to the active receptor can be easily computed: k_{off} is equal to the absolute value of the unique eigenvalue, that is, $k_{off} = k_{-3} + k_{-4}$, and the RT ($\tau$) is equal to $1/(k_{-3} + k_{-4})$.

It has been proposed that for GPCRs, the residence time is positively correlated with agonist efficacy because the longer an agonist remains bound to the receptor, the more cycles of G protein activation it can catalyze [42]. Strictly speaking, from Eq. (44) it would be more appropriate to say that the residence time of an agonist in the ligand-receptor active state rather than the residence time in the full range of

receptor conformations would be expected to be positively correlated with agonist efficacy.

3.7.3. Relaxation time of the active receptor species

Following the previous discussion, which focused on the residence time of the ligand in the ligand-receptor active state, and considering that the inclusion of R* in the two-state model of Fig. 8 implies constitutive activity of the receptor, it makes sense to propose a kinetic subscheme in which both active states of the receptor, R* and LR*, are the chemical species of interest:

$$L+R \underset{k_{-1}}{\leftarrow} L+R^* \underset{k_{-3}}{\overset{k_3}{\rightleftarrows}} LR^* \underset{k_{-4}}{\rightarrow} LR \tag{46}$$

It is worth noting that the association rate constant k_3 was included in Eq. (46) because, in the same way that LR and LR* were included in Eq. (42), we are treating R* and LR* as functionally equivalent. The corresponding two-dimensional ODE system is

$$\begin{cases} \dfrac{d[R^*]}{dt} = -(k_{-1}+k_3[L])[R^*]+k_{-3}[LR^*], \\ \dfrac{d[LR^*]}{dt} = k_3[L][R^*]-(k_{-3}+k_{-4})[LR^*]. \end{cases} \tag{47}$$

The inclusion of R* in the residence time framework has conceptual and terminological consequences. Drug-target residence time involves the dissociation of a ligand from a receptor to which it was previously bound. However, the rate constant k_{-1} involves the deactivation of a receptor species with no ligand present. Because of this, we suggest using the term relaxation time (RXT) instead of residence time (RT) when considering the lifetime of receptor species that do not involve ligand dissociation. In this way, the RXT allows for an extension of the residence time concept to situations where the focus is more on ligand function than ligand binding and can be considered a hybrid between binding kinetics and receptor functionality. It is worth noting that RXT has a resemblance to Cornish-Bowden's approach (see Appendix B). We will follow our formalism and use the symbol τ in the same way as before.

From the computations shown in Appendix D.7, we observe that two interesting limit conditions can be considered: $[L]=0$ and $[L]\to+\infty$. In the first case, the absence of ligand can arise either from a situation of basal conditions or from a process of rapid ligand elimination after ligand-receptor dissociation. In system (47), when considering $[L]=0$ under basal conditions, the RXT is equal to $1/k_{-1}$ because the only chemical species that remains is R*. On the contrary, if a fast elimination process is considered, the RXT (see Appendix D) is either $1/(k_{-3}+k_{-4})$ if $k_{-1}>k_{-3}+k_{-4}$ or $1/k_{-1}$ if $k_{-1}\le k_{-3}+k_{-4}$. Because k_{-1} is the rate constant for the decay of R* in system (47) and $k_{-3}+k_{-4}$ is the global rate constant for the decay of LR*, then the biological interpretation of these results is the following: if $k_{-1}\le k_{-3}+k_{-4}$, the decay of R* is dominant (its eigenvalue is the smallest in modulus), while if $k_{-1}>k_{-3}+k_{-4}$, then the decay of LR* is the dominant one.

On the contrary, at saturating ligand concentrations ([L] increasing indefinitely), the RXT is (see again Appendix D) $1/k_{-4}$.

Therefore, we can conclude that the RXT depends on [L], but it ranges between $1/k_{-1}$ (or $1/(k_{-3}+k_{-4})$), when no ligand is present, and $1/k_{-4}$, at saturating ligand concentrations. In the context of a functional experiment, it would be worth taking this interval into account because the expected pharmacological effect will be influenced by the RXT.

4. Discussion

4.1. Comparison with Johnson's and Cornish-Bowden's approaches

The concept of RT is frequently used in the literature but in many cases in a qualitative way. Quantitative expressions are scarce and are reduced mainly to the induced-fit model (Eq. (6)). The aim of the herein presented study is to provide a methodology for the determination of k_{off} (and the RT by its inverse) that can be of general applicability. To this end, the correspondence found with two previous studies, by Johnson and Cornish-Bowden [4,5], whose derivations are included in Appendix A and Appendix B, respectively, are a good indication of the validity of the proposal.

The expression for k_{off} obtained in [5] by setting $[S]=0$ is given in equation (A9) of Appendix A. In fact, it is a simplified version of Eq. (7), obtained through a Taylor series to eliminate the square root. This is valid, but only for chemical situations such as (6), (A1) and (23). Johnson's approach does not allow a generalization of k_{off}. However, if we focus on Eqs. (A3) and (A4), more precisely on the expression that Johnson uses for k_{off} (λ_2^J) before simplifying it and setting $[S]=0$, it can be noticed that it is the same as the formula for k_{off} that we have obtained in Eq. (24). In fact, Eq. (24) can be written as

$$k_{off} = \left.\frac{P-\sqrt{P^2-4Q}}{2}\right|_{[S]=0}, \tag{48}$$

with P and Q defined as in (A4), see Appendix A.

On the other hand, in [4], a general solution of type (13) is obtained for the conformational exchange system considered. Although an expression for k_{off} is not explicitly defined (because the model is quite general, not applied to any particular field), we can find the term "relaxation time" defined as the inverse of the coefficient (in absolute value) of the exponent of an exponential term in the analytical solution of the system. This is exactly the same as the RT that can be obtained through the eigenvalues of the system, since eigenvalues are precisely the coefficients of the exponents of the exponential terms. Thus, the expression for RT, although it is not obtained in Cornish-Bowden's approach, would be one of the relaxation times he obtained (τ_2), and k_{off} would be λ_2^C in equation (B12). Furthermore, the term "relaxation time" inspired us to extend RT to RXT in pharmacology for those cases that consider chemical species of interest with no ligand present. By doing so, our formalism gains in generalization and pharmacological applicability.

In the same way as in Johnson's approach, the value of k_{off} defined in (14) coincides with λ_2^C for $k_1=0$. This is analogous to setting $[S]=0$, because it means that association processes are omitted. Therefore, we can state that the smallest-modulus eigenvalue-based method we presented is compatible with both Johnson's and Cornish-Bowden's approaches. The only minor difference is that both λ_2^J and λ_2^C were defined positive, while we take λ_1 as the smallest-modulus negative eigenvalue and define k_{off} as its absolute value. Furthermore, it can be considered that our procedure is more general than that of Johnson's and more applicable than that of Cornish-Bowden's. Regarding the latter, while solving the system is the most complete method, it is intractable in higher dimensions and when the system is nonlinear. It is much more effective and affordable to calculate the eigenvalues and determine which one has the smallest modulus.

In both [4,43] we can observe that eigenvalues are calculated because they are the coefficients of the exponents in the exponential terms of the analytical solutions, and therefore, they are essential when solving systems; but the concept of eigenvalue itself is not mentioned at

all. Eigenvalues are known to be a source of information (stability, for instance) of an ODE system besides being just parameters of the analytical solution. This idea of taking eigenvalues as a source of information is present in [16], where the concepts of fast and slow manifolds are mentioned. The disparity in absolute value of the eigenvalues defines which ones describe slow or fast manifolds in the system. Slow manifolds are usually the ones that can be measured experimentally [12,13]. This idea supports the choice of the eigenvalue λ_1 as the source of k_{off} and, in fact, the usual formula for k_{off} in Eq. (7) is just a simplification of λ_1 for that system.

It is also worth commenting on the possible difficulties that may arise when applying this methodology to higher-dimensional examples with a large number of parameters. It may happen, then, that it is not so easy to distinguish the eigenvalue closest to zero. However, even in this case, the methodology that we propose can always be applied numerically if the values of the parameters are known, or by imposing conditions on the parameters that guarantee both that all the eigenvalues have negative real part and the detection of the eigenvalue closest to zero. We believe that it is an interesting challenge that opens new avenues for future research since it is an open question for all chemical reactions presenting a large number of agents that influence the residence time. Nevertheless, this methodology offers strong advantages: it is not necessary to calculate analytical solutions since only the eigenvalues are needed, and it is not necessary to deal with the complete original system, but only a part of it (the subsystem of interest obtained by omitting association or formation processes).

Notice also that hypotheses (H1) and (H2) are very generic and only non-generic situations are excluded. For instance, the case in which the smallest-modulus eigenvalue is real and repeated (mathematically speaking, it is said to have multiplicity 2 or greater) or the case where there are two or more pairs of complex conjugate eigenvalues with the same real part. While our methodology could also be applied, it would require a more thorough analysis to determine the combination of parameters of the system that defines the characteristic time. This analysis would imply desingularization processes of the equilibria beyond the classical linearizations. Nevertheless, all examples examined in this study clearly satisfy hypothesis (H1).

4.2. Correspondence between k_{off} and k_{cat} in enzymology

The eigenvalues method to obtain k_{off} can be extended to fields other than pharmacology because there may be parameters that, although different from k_{off} in meaning, are the same from a mathematical perspective. In enzymology, k_{cat} can be considered analogous to k_{off} in binding kinetics. The *turnover number* or *catalytic constant*, k_{cat}, is defined as the number of moles of substrate transformed into product per minute per mole of active subunit or catalytic center under optimal conditions [44]. The overall rate of reaction progress after the enzyme-substrate (ES) complex formation is quantified experimentally in terms of k_{cat}, which is a composite rate constant [45,46]. It can be stated that k_{cat} is a first-order rate constant related to the chemical steps following the formation of the ES complex, so that the rate for a generic enzymatic reaction is equal to $k_{cat}[ES]$. In the simplest case, when the ES complex breakdown generates the product P, k_{cat} is equal to k_2:

$$E+S \underset{k_{-1}}{\overset{k_1}{\rightleftarrows}} ES \xrightarrow{k_2} E+P \tag{49}$$

However, when there are more steps between the ES complex and product formation, as in

$$E+S \underset{k_{-1}}{\overset{k_1}{\rightleftarrows}} ES \underset{k_{-2}}{\overset{k_2}{\rightleftarrows}} EP \xrightarrow{k_3} E+P \tag{50}$$

k_{cat} is a function of the rate constants that appear in the sequence of chemical steps:

$$k_{cat} = \frac{k_2 k_3}{k_{-2}+k_2+k_3}. \tag{51}$$

Eq. (51) resembles the expression for k_{off} in Eq. (7), which is the simplified formula for k_{off} in two-dimensional systems given by Johnson [5]. However, at first glance, Eqs. (50) and (6) are not similar. How then are k_{cat} and k_{off} related to each other? It becomes clearer if we look at Eq. (50) backwards, since k_{cat} is a global forward rate constant (from the ES complex to product formation) and k_{off} is a global dissociation (backward) rate constant.

$$E+P \xleftarrow{k_3} EP \underset{k_2}{\overset{k_{-2}}{\rightleftarrows}} ES \tag{52}$$

Although k_{cat} and k_{off} are conceptually different, k_{cat} can be considered to play the same role as k_{off} but for product formation rather than for drug dissociation from the target. The ES complex is analogous to LR*, and because Eq. (52) does not consider the binding of the product to the enzyme, but only dissociation, what is then measured is as a "global dissociation process" of the product. The inverse of k_{cat} gives the time required for a single catalytic cycle, and this time in enzymology would be mathematically analogous to the residence time in binding kinetics.

4.3. Eigenvalues versus half-lifetime

In the experimental context, the function $\widehat{x}(t) = ae^{-bt}$ is usually used to fit data that show an apparent exponential decay of some concentration along time, $x_i(t)$. Once a and b are estimated, the half-lifetime is computed as $\ln(2)/b$ [1,47}. Note that if we had a model that perfectly explained the experimental data, we would have that

$$x_i(t) = \sum_{j=1}^{n} a_{ij} e^{-\lambda_j t}, \tag{53}$$

where a_{ij} are constant values depending on the initial concentrations $x_i(0)$ of the i-th species. In this case, the half-life ($t_{1/2}$) would be the solution of the equation $x_i(t) = x_i(0)/2$.

Our proposal consists of considering, for the generic case where hypothesis (H1) is satisfied, only the leading term of this expression, that is, the one corresponding to the smallest-modulus eigenvalue λ_1. Therefore, we consider the approximation $x_i(t) \approx a_{i1} e^{-\lambda_1 t}$.

Indeed, we note that without the hypothesis (H1), there would not be a good fit of $\widehat{x}(t) = ae^{-bt}$ to the experimental data. Then, from our approximation of $x_i(t)$, the following approximation of the half-lifetime can be obtained:

$$\widetilde{t_{\frac{1}{2}}} = \frac{ln2}{\lambda_1}. \tag{54}$$

Table 3
Comparison of residence time results obtained from $t_{\frac{1}{2}}$ and $\widetilde{t_{\frac{1}{2}}}$ for different parameter values. The ODE system for this situation is given in (17), and solutions can be seen in the graphs of Fig. 3. The value $t_{\frac{1}{2}}$ is provided by the complete analytical solution of the system and is obtained by solving numerically, while $\widetilde{t_{\frac{1}{2}}}$ is computed as $\ln(2)/\lambda_1$ by using only the dominant term of the solution, which is the exponential term with the smallest-modulus eigenvalue λ_1.

K_R	k_2 (s^{-1})	Residence time using $\widetilde{t_{\frac{1}{2}}}$ (s)	Residence time using $t_{\frac{1}{2}}$ (s)
0.2	0.5	68.5410	68.2344
	5	60.8356	60.8323
	50	60.0834	60.0833
0.02	0.5	608.3562	607.8975
	5	519.8076	519.8023
	50	510.9804	510.9804

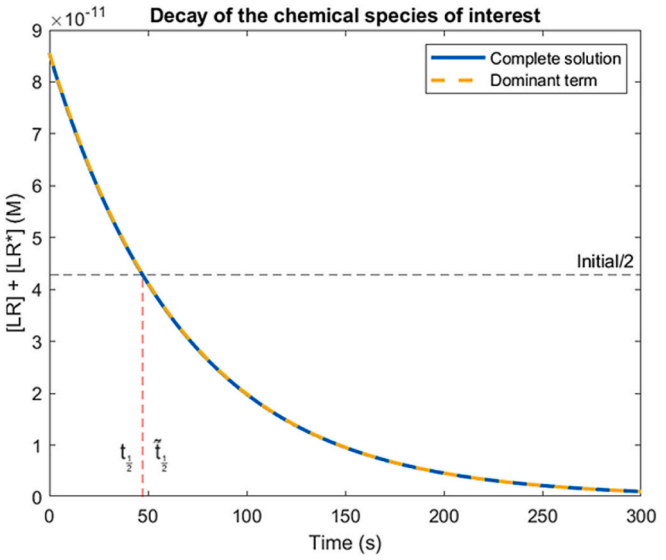

Fig. 9. Comparison between the half-lifetime $t_{\frac{1}{2}}$ and the half-lifetime $\widetilde{t_{\frac{1}{2}}}$ computed from the smallest-modulus eigenvalue. The chemical model used for this comparison is represented in Eq. (6) when $k_1 = 0$, that is, when there is no association of the ligand, and the system provides the decay of the ligand-receptor complexes previously formed. The corresponding ODE system is (17). Parameter values are $k_{-1} = 0.1\ s^{-1}$, $k_2 = 0.5\ s^{-1}$, $K_R = 0.2$ and $k_{-2} = k_2\ K_R$, and the initial condition is the equilibrium point when association is considered. The blue curve represents the complete analytical solution for this situation, which has two exponential terms ($C_1e^{-\lambda_1 t} + C_2e^{-\lambda_2 t}$) and gives $t_{\frac{1}{2}}$ by graphical calculation; while the red curve is a plot of only the dominant term of the solution: the exponential term with the smallest-modulus eigenvalue λ_1, which gives $\widetilde{t_{\frac{1}{2}}}$ as ln(2)/ λ_1.

For the sake of comparison, we have computed both residence times (obtained from $t_{\frac{1}{2}}$ and $\widetilde{t_{\frac{1}{2}}}$, respectively, by dividing by ln2) for all situations described in Fig. 3. Results are shown in Table 3. It can be seen that the approximation defined in Eq. (54) is very accurate: there are small differences (below 0.5 %) as shown by the example in Fig. 9.

The above observation is equivalent to saying that, usually, behind the apparent exponential decay of the experimental points there may not be a single exponential expression ($Ce^{-\lambda t}$), but a linear combination of them ($C_1e^{-\lambda_1 t} + C_2e^{-\lambda_2 t} + \cdots$). However, if $C_1e^{-\lambda_1 t}$ is the leading term under hypothesis (H1), then it is well fit by a single exponential. It is usual in the literature to perform fittings to mono and biexponential curves [2,16,48,49], although the purpose is to find the parameter values of the model (such as rate constants) rather than the RT, except for those cases where calculation of the RT is immediate as in Eq. (1). The aim of the above comparison of half-lives is to show that the eigenvalue of the leading term provides an accurate approximation to obtain the RT, thus being an excellent value to take as a theoretical reference for comparison with the result of an experiment. It should be noted that, as a complement to empirical data fitting, providing the herein presented expression for the RT offers the possibility of mechanism-based modeling of experimental conditions.

In Sections 3.3 and 3.5, we present two examples of residence time estimation obtained from experimental data of the temporal course [16,36]. The example in Section 3.5 [36] is considered ideal for the methodology proposed here. In particular, in Fig. 7b, we observe that the result of the fitting to a mechanistically predicted biphasic decay is not different from that of an empirical monophasic decay. The reason is that one of the exponential terms of the biphasic decay is dominant over the other, so that the other is masked and is not detectable. For this type of situation, it is recommended for simplicity to fit the data with a monophasic exponential decay, bearing in mind that the mechanism-based expression for k_{off} comes from the dominant term of a biphasic decay which depends on several rate constants of the model (see Appendix D.4).

On the contrary, the example included in Section 3.3 is not ideal: the difference between the two eigenvalues is not very large, so the dominant term does not mask the other, especially at the beginning (see Fig. 4). Therefore, it would be incorrect to fit the data with a monophasic exponential decay, which can be easily verified with the values of Table 1. The fitting to a monophasic decay yields a RT of 85.5 min, while the smallest-modulus eigenvalue of the biphasic decay gives 142.8 min, which is very different. Taking into account that the best fitting function for this case is the biphasic decay, since the dominant term does not mask the other exponential term, another problem would be deciding which is the RT: the one that comes from the dominant exponential term, the other, or some type of average between them. If the dominant term is chosen, the RT will be 142.8 min, while selecting the other term results in a RT of 30.3 min. To address this issue, consider the following analogy: if a cinema is showing two movies simultaneously in two different rooms (one lasting two hours and the other an hour and a half) it cannot close until the longer movies ends. Similarly, in a scientific context, imagine a drug that binds to two different receptor conformations: one for 60 min and the other for 10 min. Choosing a residence time (RT) shorter than 60 min would be incorrect, as it would ignore the longer binding event (just as closing the cinema before the longest movies ends would be premature). Thus, even in non-ideal cases, the dominant term still defines the correct RT, as it captures the slowest, and therefore most limiting, timescale of the system [50].

4.4. Eigenvalues versus mean residence time

As stated in the introduction, the MRT is a mathematical expression for the RT in a pharmacokinetic context that can also be applied to binding kinetics by making some analogies. In this section, we want to show that working with the MRT formula, already shown in Eq. (9), is more tedious, has limitations and, moreover, if the condition is met that one of the eigenvalues is much smaller than the others, then the formula for the MRT gives $1/\lambda_1$ (in absolute value), which is the result proposed in this article for the RT.

To be applicable in a pharmacokinetic context, the MRT formula needs an analytical expression for the concentration of the ligand in all the compartments that have an elimination rate constant. If this idea is translated to the world of binding kinetics, then the "compartments" become ligand-receptor complexes, and the "elimination" rate constants become dissociation rate constants.

Thus, we obtain the MRT for three cases: A) simple dissociation (Eq. (1) with $k_1 = 0$), B) dissociation after receptor deactivation (Eq. (6) with $k_1 = 0$) and C) dissociation whether the receptor was previously activated or not (Eq. (42)). It is worth mentioning that all three examples are linear. Therefore, it is possible to obtain the analytical solution required for the MRT formula (9) and we can then compare with the analytical results obtained from the eigenvalues method. However, as mentioned above, the MRT may not be applicable in more complex situations.

In Case A, the MRT is $1/\lambda_1$, while in Cases B and C, more complex expressions are obtained:

$$MRT_B = \frac{\frac{C_1}{\lambda_1^2} + \frac{C_2}{\lambda_2^2}}{\frac{C_1}{\lambda_1} + \frac{C_2}{\lambda_2}}, \tag{55}$$

$$MRT_C = \frac{\frac{k_{-1}C_1 + k_{-3}D_1}{\lambda_1^2} + \frac{k_{-1}C_2 + k_{-3}D_2}{\lambda_2^2}}{\frac{k_{-1}C_1 + k_{-3}D_1}{\lambda_1} + \frac{k_{-1}C_2 + k_{-3}D_2}{\lambda_2}}. \tag{56}$$

Nevertheless, it can be shown that all these expressions of MRT can be approximated by $1/\lambda_1$ under hypothesis (H1), see the proof in Appendix C. It is important to note that these λ_1 values are different in each case since they are dealing with different chemical situations. For

Case A, $\lambda_1 = k_{-1}$; for Case B, λ_1 has the following expression:

$$\lambda_1 = \frac{k_{-1} + k_{-2} + k_2 - \sqrt{(k_{-1} + k_{-2} + k_2)^2 - 4k_{-1}k_{-2}}}{2}, \quad (57)$$

and for Case C, λ_1 has the following expression:

$$\lambda_1 = \frac{a - \sqrt{a^2 - 4(k_{-2}k_{-4} + k_{-3}(k_{-2} + k_4))}}{2}, \quad (58)$$

where $a = k_{-2} + k_{-4} + k_4 + k_{-3}$.

The calculation of the MRT by Plusquellec and Houin [7] is applicable (in principle) to any system, but it has a notable limitation: the analytical solution of the ODE system is needed, otherwise the MRT cannot be obtained analytically. It is usually easy to study and work with linear systems, as well as to obtain analytical solutions either using the Laplace transform [51] or not. However, when dealing with nonlinear systems, obtaining an analytical solution is clearly more difficult or even impossible, and this is the reason why nonlinear systems are studied by performing different approximations to make them linear and solving them under some constraints. This is not a problem if we only calculate the RT through the eigenvalues of the system, because the analytical solution is not needed. Eigenvalues can be obtained for every system, no matter if it is linear or nonlinear. Therefore, the eigenvalue-based method we present here is more practical and easier to implement.

5. Conclusions

We have presented a general mathematical formalism for residence time quantification that is based on the concept of the smallest-modulus eigenvalue of a dynamical system. The resulting expressions are consistent with those mostly found in the literature and, importantly, can be extended to other pharmacological systems in a general way: an application to a two-state receptor model is shown, as well as homodimeric, homotetrameric and heterodimeric receptors. Moreover, we apply this residence time definition to a system where rebinding occurs and we consider that the key for this case is to put the focus on the proximity of the receptor or the cell, rather than only on the receptor itself. Furthermore, we propose an extension of residence time to relaxation time for those cases where one is only interested in those receptor species responsible for the pharmacological effect, whether they have bound ligand or not. This generalized and widely applicable formulation of residence time / relaxation time is expected to be of help for drug discovery and development.

CRediT authorship contribution statement

Antonio J. Ortiz: Writing – original draft, Methodology, Investigation, Formal analysis, Conceptualization. **David Romero:** Writing – review & editing, Writing – original draft, Methodology, Investigation, Formal analysis, Conceptualization. **Antoni Guillamon:** Writing – review & editing, Writing – original draft, Supervision, Methodology, Investigation, Formal analysis, Conceptualization. **Jesús Giraldo:** Writing – review & editing, Writing – original draft, Supervision, Methodology, Investigation, Funding acquisition, Formal analysis, Conceptualization.

Declaration of competing interest

The authors declare that they have no known competing financial interests or personal relationships that could have appeared to influence the work reported in this paper.

Acknowledgements

This project has received funding from the European Union's Horizon2020 research and innovation programme under grant agreement No 848068. This publication reflects only the authors' view and the European Commission is not responsible for any use that may be made of the information it contains. This work is partially supported by the grants PID2020-119136RB-I00, PID-2021-122954NB-I00 and the Severo Ochoa and María de Maeztu Programs for Centers and Units of Excellence in R&D (CEX2020-001084-M) funded by MCIN/AEI/ 10.13039/501100011033 and by ERDF "A way of making Europe", and by the AGAUR grant 2021-SGR-01039. AJO is funded by FPI fellowship (PRE2021-100772) associated to PID2020-119136RB-I00 grant. We thank Dr Adriaan IJzerman from Leiden University for providing us the experimental data of 2 out of 5 independent experiments, which were used to depict the exponential decays in Section 3.3.

Appendix A. Johnson's approach to k_{off}

In [5], an enzymatic system showing a mechanistic resemblance with Eq. (6) was presented:

$$E + S \underset{k_{-1}}{\overset{k_1}{\rightleftarrows}} ES \underset{k_{-2}}{\overset{k_2}{\rightleftarrows}} EX \quad (A1)$$

Scheme (A1) shows the binding of a substrate S to an enzyme E to form the substrate-enzyme complex ES in dynamic equilibrium with EX, with X representing a transition state of the substrate in the enzymatic process.

The general solution for the concentration of the chemical species in Eq. (A1) was proposed to be

$$B(t) = A_1 e^{-\lambda_1 t} + A_2 e^{-\lambda_2 t} + D, \quad (A2)$$

with B(t) representing the variation along time of either of the E, S, ES or EX chemical species. The mathematical form of B(t) is a linear combination of decreasing exponentials, where $\lambda_{1,2}$ (defined as positive values) are the coefficients of the exponents. A_1 and A_2 are the amplitudes of the exponential function and D is a constant. The expressions for parameters λ_1 and λ_2 are:

$$\lambda_1^J := \frac{P + \sqrt{P^2 - 4Q}}{2}, \lambda_2^J := \frac{P - \sqrt{P^2 - 4Q}}{2}, \quad (A3)$$

Where

$$P = k_1[S] + k_{-1} + k_2 + k_{-2}, Q = k_1[S](k_2 + k_{-2}) + k_{-1}. \quad (A4)$$

The superscript J is used to indicate that is a Johnson's result.

A Taylor series approximation for the square root followed [5]. To do this, the roots in (A3) are rearranged as

$$\sqrt{P^2 - 4Q} = P\sqrt{1 - \frac{4Q}{P^2}}. \tag{A5}$$

The square root in (A5) has the form of the function $\sqrt{1-x}$, which can be approximated by Taylor series around x = 0 provided that $P^2 \gg 4Q$. This inequality relies on the differences in orders of magnitude between forward (k_1 and k_2) and backward (k_{-1} and k_{-2}) microscopic rate constants, being the backward ones much smaller than the forward ones.

The first order expansion of $\sqrt{1-x}$ is $1 - \frac{x}{2}$ and so,

$$\sqrt{1 - \frac{4Q}{P^2}} \approx 1 - \frac{2Q}{P^2} \tag{A6}$$

up to first order. The first neglected term is the quadratic term $-2Q^2/P^4$.Therefore, λ_1^J can be approximated by

$$\lambda_1^{J^*} := \frac{P\left(1 + \left(1 - \frac{2Q}{P^2}\right)\right)}{2} = \frac{2P\left(1 - \frac{Q}{P^2}\right)}{2} = P - \frac{Q}{P}, \tag{A7}$$

where the asterisk is used to denote approximation. Since, $P^2 \gg 4Q$ implies that $P \gg Q/P$, it can be further approximated:

$$\lambda_1^{J^*} \approx P = k_1[S] + k_{-1} + k_2 + k_{-2} \tag{A8}$$

On the other hand,

$$\lambda_2^{J^*} := \frac{P\left(1 - \left(1 - \frac{2Q}{P^2}\right)\right)}{2} = \frac{Q}{P} = \frac{k_1[S](k_2 + k_{-2}) + k_{-1}k_{-2}}{k_1[S] + k_{-1} + k_2 + k_{-2}}, \tag{A9}$$

Finally, assuming that there is no association of the substrate to the enzyme, [S] is considered to be equal to 0 in $\lambda_2^{J^*}$, which provides Johnson's approximation of k_{off}:

$$k_{off} = \lambda_2^{J^*}([S] = 0) = \frac{k_{-1}k_{-2}}{k_{-1} + k_2 + k_{-2}}. \tag{A10}$$

B. Cornish-Bowden's approach to conformational equilibria

Cornish-Bowden [4] considers the chemical system

$$X_0 \underset{k_{-1}}{\overset{k_1}{\rightleftarrows}} X_1 \underset{k_{-2}}{\overset{k_2}{\rightleftarrows}} X_2 \tag{B1}$$

In contrast with the process presented in Eq. (A1) [5] and that presented in Eq. (6), there is no ligand–protein binding process but just the interconversion between three generic chemical species X_0, X_1 and X_2. Eq. (B1) can be converted into (A1) or (6) by making k_1 in (B1) equal to $k_1[S]$ or $k_1[L]$, respectively.

The ODE system that describes the variation with time of the concentration of each chemical species is the following:

$$\begin{cases} \frac{dx_0}{dt} = k_{-1}x_1 - k_1x_0, \\ \frac{dx_1}{dt} = k_1x_0 - (k_{-1} + k_{-2})x_1 + k_{-2}x_2, \end{cases} \tag{B2}$$

where $x_2 = x_{tot} - x_0 - x_1$.

Then, some substitutions and rearrangements were made to reduce the system to a single differential equation, which was solved to obtain the general solution for X_0, X_1 and X_2.

First, by substituting x_2 in the second equation of (B2), we get:

$$\frac{dx_1}{dt} = k_1x_0 - (k_{-1} + k_{-2})x_1 + k_{-2}(x_{tot} - x_0 - x_1) = (k_1 - k_{-2})x_0 - (k_{-1} + k_{-2} + k_2)x_1 + k_{-2}x_{tot}. \tag{B3}$$

Then, dx_0/dt is differentiated to obtain d^2x_0/dt^2, and dx_1/dt is substituted in d^2x_0/dt^2 according to (B3):

$$\frac{d^2x_0}{dt^2} = -k_1\frac{dx_0}{dt} + k_{-1}\frac{dx_1}{dt} = -k_1\frac{dx_0}{dt} + k_{-1}(k_1 - k_{-2})x_0 - k_{-1}(k_{-1} + k_{-2} + k_2)x_1 + k_{-1}k_{-2}x_{tot}. \tag{B4}$$

The variable x_1 can be eliminated from d^2x_0/dt^2 if $k_{-1}x_1$ is isolated in the first equation of (B2) and the resulting expression is substituted in d^2x_0/dt^2.

$$\frac{dx_0}{dt}+k_1x_0=k_{-1}x_1,$$

$$\frac{d^2x_0}{dt^2}=-k_1\frac{dx_0}{dt}+k_{-1}(k_1-k_{-2})x_0-(k_{-1}+k_{-2}+k_2)\left(\frac{dx_0}{dt}+k_1x_0\right)+k_{-1}k_{-2}x_{tot}. \tag{B5}$$

Rearranging terms, the following second order ODE is obtained:

$$\frac{d^2x_0}{dt^2}+(k_1+k_{-1}+k_{-2}+k_2)\frac{dx_0}{dt}+(k_{-1}k_{-2}+k_1k_2+k_1k_{-2})x_0=k_{-1}k_{-2}x_{tot}. \tag{B6}$$

If we compare the coefficients of dx_0/dt and x_0 to P and Q expressions (A4), it can be seen that they are equal taking into account that k_1 is multiplied by [S] or [L] when the first reaction is a binding process. By this way, equation (B6) can be rewritten as:

$$\frac{d^2x_0}{dt^2}+P\frac{dx_0}{dt}+Qx_0=R. \tag{B7}$$

It was stated [4] that the solution of equation (B7) is a linear combination of decreasing exponential functions, but instead of denoting the coefficients of the exponentials as $\lambda_{1,2}$ as in [5], they were denoted as $1/\tau_{1,2}$. $\tau_{1,2}$ were referred as the relaxation constants of the exponentials, and the negative sign in the exponentials was included, so that the expressions for $1/\tau_{1,2}$ are positive:

$$x_0(t)=x_{0eq}+A_1e^{\frac{-t}{\tau_1}}+A_2e^{\frac{-t}{\tau_2}}. \tag{B8}$$

It was not described how the relaxation times from the second order ODE were obtained, but the procedure is described here. First, we suppose that the solution is a decreasing exponential, and substitute this proposal in (B7) in its homogeneous form, or in other words, setting the expression equal to 0 instead of R:

$$x_0=Ae^{-\lambda t}\frac{dx_0}{dt}=-\lambda Ae^{-\lambda t}\frac{d^2x_0}{dt^2}=\lambda^2Ae^{-\lambda t}, \tag{B9}$$

$$\lambda^2Ae^{-\lambda t}-P\lambda Ae^{-\lambda t}+QAe^{-\lambda t}=0. \tag{B10}$$

Since neither the exponentials nor A can be 0, (B10) can be simplified to a second degree equation and two values of λ are obtained (which are equal to the reciprocal of relaxation times). Superscript C is used to indicate that is Cornish-Bowden's result, to distinguish between authors:

$$\lambda^2-P\lambda+Q=0, \tag{B11}$$

$$\lambda_1^C:=\frac{P+\sqrt{P^2-4Q}}{2}=\frac{1}{\tau_1}\lambda_2^C:=\frac{P-\sqrt{P^2-4Q}}{2}=\frac{1}{\tau_2}. \tag{B12}$$

Of note, an expression for k_{off} was not obtained in [4], which is logical since no binding was included in the system (it is a general situation). However, the applied procedure is relevant as a reference for the methods here developed.

C. General proof of MRT ≈ λ_1 if the solution of the system is a linear combination of decreasing exponentials

In Cases A, B and C in Section 4.4., an expression for MRT is obtained. However, for these three cases and, in general, considering a system where the analytical solution $x_i(t)$, for i = 1,…,n, consists of a linear combination of m decreasing exponentials, it can be shown that MRT ≈ $1/\lambda_1$, where λ_1 is the absolute value of the smallest modulus eigenvalue of the system for each case. Let us prove it: set

$$x_i(t)=\sum_{j=1}^{m}C_{ij}e^{-\lambda_jt}. \tag{C1}$$

Substituting (C1) in (8), we obtain the following density function:

$$\phi(t)=\frac{\sum_{i=1}^{n}k_i\sum_{j=1}^{m}C_{ij}e^{-\lambda_jt}}{\int_0^\infty\sum_{i=1}^{n}k_i\sum_{j=1}^{m}C_{ij}e^{-\lambda_jt}dt}=\frac{\sum_{i=1}^{n}k_i\sum_{j=1}^{m}C_{ij}e^{-\lambda_jt}}{\sum_{i=1}^{n}k_i\sum_{j=1}^{m}\frac{C_{ij}}{\lambda_j}}, \tag{C2}$$

and then, MRT is obtained from the density function by calculating the mean value:

$$MRT=\int_0^\infty t\cdot\frac{\sum_{i=1}^{n}k_i\sum_{j=1}^{m}C_{ij}e^{-\lambda_jt}}{\sum_{i=1}^{n}k_i\sum_{j=1}^{m}\frac{C_{ij}}{\lambda_j}}dt=\frac{\int_0^\infty t\cdot\sum_{i=1}^{n}k_i\sum_{j=1}^{m}C_{ij}e^{-\lambda_jt}dt}{\sum_{i=1}^{n}k_i\sum_{j=1}^{m}\frac{C_{ij}}{\lambda_j}}=\frac{\sum_{i=1}^{n}k_i\sum_{j=1}^{m}C_{ij}\int_0^\infty te^{-\lambda_jt}dt}{\sum_{i=1}^{n}k_i\sum_{j=1}^{m}\frac{C_{ij}}{\lambda_j}}=\frac{\sum_{i=1}^{n}k_i\sum_{j=1}^{m}\frac{C_{ij}}{\lambda_j^2}}{\sum_{i=1}^{n}k_i\sum_{j=1}^{m}\frac{C_{ij}}{\lambda_j}}. \tag{C3}$$

After that, we multiply the numerator and the denominator by λ_1^2 and, up to this point, we have not used the hypothesis that λ_1 is much smaller than the rest of the eigenvalues (as assumed in this article). Under this hypothesis, it can be observed that only the first term of the sums in j is relevant and the rest can be obviated because their contribution is small compared to the first one:

$$MRT\left(\lambda_1 \ll \lambda_{j>1}\right) = \frac{\lambda_1^2 \sum_{i=1}^{n} k_i \sum_{j=1}^{m} \frac{C_{ij}}{\lambda_j^2}}{\lambda_1^2 \sum_{i=1}^{n} k_i \sum_{j=1}^{m} \frac{C_{ij}}{\lambda_j}} = \frac{\sum_{i=1}^{n} k_i \sum_{j=1}^{m} \frac{\lambda_1^2 C_{ij}}{\lambda_j^2}}{\sum_{i=1}^{n} k_i \sum_{j=1}^{m} \frac{\lambda_1^2 C_{ij}}{\lambda_j}} = \frac{\sum_{i=1}^{n} k_i \sum_{j=1}^{m} \frac{\lambda_1^2 C_{ij}}{\lambda_j^2}}{\sum_{i=1}^{n} k_i \sum_{j=1}^{m} \frac{\lambda_1^2 C_{ij}}{\lambda_j}} \approx \frac{\sum_{i=1}^{n} k_i C_{i1}}{\sum_{i=1}^{n} k_i \lambda_1 C_{i1}} = \frac{\sum_{i=1}^{n} k_i C_{i1}}{\lambda_1 \sum_{i=1}^{n} k_i C_{i1}} = \frac{1}{\lambda_1}, \tag{C4}$$

which coincides with the definition of residence time proposed in this article.

D. Mathematical computations to obtain the residence times provided in the results

This appendix contains mathematical technicalities that lead to the RT expressions in the main text.

D.1. The conformational induction model (see Section 3.2)

Let us define the right-hand side parts of system (17), for the two chemical species of interest, LR and LR* as

$$\begin{cases} F([\mathrm{LR}], [\mathrm{LR}^*]) := -(k_{-1} + k_2)[LR] + k_{-2}[\mathrm{LR}^*], \\ G([\mathrm{LR}], [\mathrm{LR}^*]) := k_2[LR] - k_{-2}[\mathrm{LR}^*]. \end{cases} \tag{D1}$$

To obtain the eigenvalues of the system, we compute the Jacobian matrix, formed by the partial derivatives of F and G,

$$J = \begin{pmatrix} -(k_{-1} + k_2) & k_{-2} \\ k_2 & -k_{-2} \end{pmatrix}, \tag{D2}$$

and then obtain the roots (zeros) of the *characteristic polynomial* $P(\lambda) = \det(J - \lambda \mathrm{Id})$, where Id is the identity matrix. Therefore, they are obtained by solving

$$\begin{vmatrix} -(k_{-1} + k_2) - \lambda & k_{-2} \\ k_2 & -k_{-2} - \lambda \end{vmatrix} = 0, \tag{D3}$$

which leads to the degree-two polynomial

$$\lambda^2 + (k_{-1} + k_{-2} + k_2)\lambda + k_{-1}k_{-2} = 0. \tag{D4}$$

The roots of the polynomial are, then,

$$\lambda_m := \frac{-(k_{-1} + k_{-2} + k_2) - (-1)^m \sqrt{(k_{-1} + k_{-2} + k_2)^2 - 4k_{-1}k_{-2}}}{2}, m = 1, 2. \tag{D5}$$

Note that we could have also obtained expression (D5) directly from (21) since the determinant and the trace of the matrix (D2) are $det(J) = k_{-1}k_{-2}$ and $tr(J) = -(k_{-1} + k_{-2} + k_2)$.

Observe also that our procedure applies for this model since the expression inside the square root is always positive and so hypothesis (H1) is fulfilled; indeed, notice that

$$(k_{-1} + k_{-2} + k_2)^2 - 4k_{-1}k_{-2} = (k_{-1} - k_{-2} + k_2)^2 + 4k_{-2}k_2, \tag{D6}$$

which is positive since all constants k_j are positive. Moreover, we have that $\lambda_2 < \lambda_1 < 0$, which implies that the equilibrium is an attractor, and that the smallest-modulus eigenvalue is λ_1. In fact, it is a global attractor [8] since system (17) is linear, that is, all solutions of the system tend to the equilibrium regardless of the initial concentrations of the species. Therefore, we conclude that

$$k_{off} = |\lambda_1| = \frac{(k_{-1} + k_{-2} + k_2) - \sqrt{(k_{-1} + k_{-2} + k_2)^2 - 4k_{-1}k_{-2}}}{2}. \tag{D7}$$

Equation (D7) corresponds to equation (24) in the main text.

D.2. The doubly and singly-occupied homodimer model (see Section 3.4.1.2)

For the doubly and singly-occupied homodimer model ODE system (32), its associated Jacobian matrix is

$$J = \begin{pmatrix} -2k_{-2} & 0 \\ 2k_{-2} & -k_{-1} \end{pmatrix} \tag{D8}$$

whose eigenvalues are $\lambda_1 = -2k_{-2}$ and $\lambda_2 = -k_{-1}$.

D.3. The homotetrameric receptor model (see Section 3.4.2)

The linear ODE sytem corresponding to the homotetrameric receptor model is given by

$$\begin{cases} \dfrac{d[L_4R_4]}{dt} = -4k_{-4}[L_4R_4], \\ \dfrac{d[L_3R_4]}{dt} = 4k_{-4}[L_4R_4] - 3k_{-3}[L_3R_4], \\ \dfrac{d[L_2R_4]}{dt} = 3k_{-3}[L_3R_4] - 2k_{-2}[L_2R_4], \\ \dfrac{d[LR_4]}{dt} = 2k_{-2}[L_2R_4] - k_{-1}[LR_4]. \end{cases} \tag{D9}$$

Thus, its associated Jacobian matrix is

$$J = \begin{pmatrix} -4k_{-4} & 0 & 0 & 0 \\ 4k_{-4} & -3k_{-3} & 0 & 0 \\ 0 & 3k_{-3} & -2k_{-2} & 0 \\ 0 & 0 & 2k_{-2} & -k_{-1} \end{pmatrix} \tag{D10}$$

and the eigenvalues λ are the roots of the characteristic polynomial of degree four:

$$(-4k_{-4} - \lambda)(-3k_{-3} - \lambda)(-2k_{-2} - \lambda)(-k_{-1} - \lambda) = 0 \tag{D11}$$

Solving for λ, four eigenvalues are obtained: $\lambda_1 = -4k_{-4}$, $\lambda_2 = -3k_{-3}$, $\lambda_3 = -2k_{-2}$ and $\lambda_4 = -k_{-1}$. Observe that the triangular structure of the Jacobian matrix (D10) is maintained for homomers with n protomers, giving

$$\tau = \max_{m=1,\cdots,n} \left\{ \frac{1}{mk_{-m}} \right\}. \tag{D12}$$

D.4. The allosteric ternary complex model (see Section 3.5)

The nonlinear ODE system corresponding to the Eq. (38) is:

$$\begin{cases} \dfrac{d[AR]}{dt} = k_{-3}[ARB] - k_3[B][AR] - k_{-1}[AR], \\ \dfrac{d[ARB]}{dt} = k_3[B][AR] - (k_{-3} + k_{-4})[ARB]. \end{cases} \tag{D13}$$

The associated Jacobian matrix is:

$$J = \begin{pmatrix} -k_3[B] - k_{-1} & k_{-3} \\ k_3[B] & -k_{-3} - k_{-4} \end{pmatrix}, \tag{D14}$$

which leads to:

$$tr(J) = -(k_3[B] + k_{-1} + k_{-3} + k_{-4}),\ det(J) = k_{-4}k_3[B] + k_{-1}k_{-3} + k_{-1}k_{-4}. \tag{D15}$$

The Jacobian matrix (D14) depends on the free concentration of B, so the matrix needs to be evaluated for a value of [B]. If ligand B is in excess with respect to the total receptor concentration, then [B] is approximately constant and equal to its total amount [B_{tot}]. If it is not in excess, [B] has a more complex expression. However, for the purpose of this section it is not necessary to go into these details: it is enough to know that [B] is not a variable, but a fixed value in this subsystem of interest.

The eigenvalues and the expression for k_{off} can be obtained plugging the expressions in (D15) into (21) and (22), respectively. Notice that we are under hypothesis (H1) since.

$$tr(J)^2 - 4\det(J) = (k_3[B] + k_{-1} + k_{-3} + k_{-4})^2 - 4(k_{-4}k_3[B] + k_{-1}k_{-3} + k_{-1}k_{-4}) = (k_3[B] + k_{-1} - k_{-3} - k_{-4})^2 + 4k_3k_{-4}[B] > 0. \tag{D16}$$

For the RT of ligand A to be higher in the presence of B, the k_{off} when A is alone must be higher. That is,

$$\frac{-tr(J) - \sqrt{tr(J)^2 - 4\det(J)}}{2} < k_{-1} \tag{D17}$$

must be satisfied. Working on inequation (D17) and simplifying, the following condition is obtained:

$$k_{-4} < k_{-1} \Leftrightarrow \alpha_- < 1 \tag{D18}$$

D.5. The rebinding case model (see Section 3.6)

The nonlinear ODE system corresponding to the rebinding model (40) is written as

$$\begin{cases} \dfrac{d[L]}{dt} = -k_1[L]([R_{tot}] - [LR]) - k_{el}[L] + k_{-1}[LR], \\ \dfrac{d[LR]}{dt} = k_1[L]([R_{tot}] - [LR]) - k_{-1}[LR]. \end{cases} \tag{D19}$$

Note that (D19) is nonlinear because of the factors [L][LR].

In particular, the Plusquellec and Houin approach for finding the MRT explained in (9) cannot be applied because we cannot find an explicit general expression for the solution. In contrast, it is straightforward to find the smallest-modulus eigenvalue and apply our methodology. Let us consider the Jacobian matrix associated to the system (D19):

$$J([L],[LR]) = \begin{pmatrix} -k_1[R_{tot}] - k_{el} + k_1[LR] & k_1[L] + k_{-1} \\ k_1[R_{tot}] - k_1[LR] & -k_1[L] - k_{-1} \end{pmatrix}. \tag{D20}$$

Due to the nonlinearity of the system, it depends on [L] and [LR] and therefore needs to be evaluated at some point before continuing with the protocol: it is easy to prove that [L] = [LR] = 0 is the only possibility for an equilibrium of the system. At this equilibrium point, the Jacobian matrix becomes.

$$J([L]=0,[LR]=0) = \begin{pmatrix} -k_1[R_{tot}] - k_{el} & k_{-1} \\ k_1[R_{tot}] & -k_{-1} \end{pmatrix} \tag{D21}$$

The determinant and the trace of J are:

$$det(J(0,0)) = k_{el}k_{-1},\ tr(J(0,0)) = -(k_1[R_{tot}] + k_{el} + k_{-1}). \tag{D22}$$

The expression of k_{off} for the ligand inside the cell (or in the vicinity of the receptor) for this case can be computed as in equation (22) with the determinant and the trace obtained in (D22):

$$k_{off} = |\lambda_1| = \frac{k_1[R_{tot}] + k_{el} + k_{-1} - \sqrt{(k_1[R_{tot}] + k_{el} + k_{-1})^2 - 4k_{el}k_{-1}}}{2} \tag{D23}$$

Equation (D23) corresponds to equation (41) in the main text. Notice that we are under hypothesis (H1) since

$$(k_1[R_{tot}] + k_{el} + k_{-1})^2 - 4k_{el}k_{-1} = (k_1[R_{tot}] + k_{el} - k_{-1})^2 + 4k_1k_{-1}[R_{tot}] > 0. \tag{D24}$$

D.6. Residence time for ligand-receptor complexes (see Section 3.7.1)

The two-dimensional ODE system for LR and LR* dynamics is written as

$$\begin{cases} \dfrac{d[LR]}{dt} = -(k_{-2} + k_4)[LR] + k_{-4}[LR^*], \\ \dfrac{d[LR^*]}{dt} = k_4[LR] - (k_{-3} + k_{-4})[LR^*]. \end{cases} \tag{D25}$$

The Jacobian matrix is obtained straightforwardly from system (D25):

$$J = \begin{pmatrix} -(k_{-2} + k_4) & k_{-4} \\ k_4 & -(k_{-3} + k_{-4}) \end{pmatrix}. \tag{D26}$$

The determinant and the trace of J are:

$$tr(J) = -(k_{-2} + k_{-3} + k_{-4} + k_4),\quad det(J) = k_{-2}k_{-4} + k_{-2}k_{-3} + k_{-3}k_4. \tag{D27}$$

Then, k_{off} is computed as in (22) with the trace and the determinant (D27). Notice that we are under hypothesis (H1) since

$$(k_{-2} + k_{-3} + k_{-4} + k_4)^2 - 4(k_{-2}k_{-4} + k_{-2}k_{-3} + k_{-3}k_4) = (k_{-2} - k_{-3} - k_{-4} + k_4)^2 + 4k_4k_{-4} > 0 \tag{D28}$$

D.7. Relaxation time of the active receptor species (see Section 3.7.3)

From the Eq. described in (46), we are led to equation (47). Proceeding as in the previous examples, we get.

$$tr(J) = -(k_{-1} + k_{-3} + k_{-4} + k_3[L]),\quad det(J) = k_{-1}k_{-3} + k_{-1}k_{-4} + k_{-4}k_3[L]. \tag{D29}$$

Notice that we are under hypothesis (H1) since.

$$(k_{-1} + k_{-3} + k_{-4} + k_3[L])^2 - 4(k_{-1}k_{-3} + k_{-1}k_{-4} + k_{-4}k_3[L]) = (k_{-1} - k_{-3} - k_{-4} + k_3[L])^2 + 4k_3k_{-3}[L] > 0. \tag{D30}$$

The RXT is computed plugging the expressions from (D29) into (22) and, hence, the RXT depends on the free ligand concentration.

In system (47), when considering [L] = 0 under basal conditions, the RXT is equal to $1/k_{-1}$ because the only chemical species that remains is R*. On the contrary, if a fast elimination process is considered, the RXT can be obtained by setting [L] = 0 in tr(J) and det(J) (D29) and then simplifying τ, the inverse of the expression (22), to yield the following:

$$\tau|_{[L]=0} = \frac{2}{-tr(J) - \sqrt{tr(J)^2 - 4det(J)}}\Bigg|_{[L]=0} = \frac{2}{k_{-1}+k_{-3}+k_{-4} - \sqrt{(k_{-1}+k_{-3}+k_{-4})^2 - 4(k_{-1}k_{-3}+k_{-1}k_{-4})}} = \frac{2}{k_{-1}+k_{-3}+k_{-4} - \sqrt{(k_{-1}-k_{-3}-k_{-4})^2}}$$

$$= \frac{2}{k_{-1}+k_{-3}+k_{-4} - |k_{-1}-k_{-3}-k_{-4}|} = \begin{cases} \frac{1}{k_{-3}+k_{-4}} if \;\; k_{-1} > k_{-3}+k_{-4}, \\ \frac{1}{k_{-1}} if \;\; k_{-1} \le k_{-3}+k_{-4}. \end{cases} \tag{D31}$$

At saturating ligand concentrations, the limit of τ as [L] increases can be calculated (by multiplying and dividing the inverse of (22) by the conjugate of the denominator):

$$\lim_{[L]\to+\infty} \tau = \lim_{[L]\to+\infty} \frac{2}{-tr(J) - \sqrt{tr(J)^2 - 4det(J)}} = \lim_{[L]\to+\infty} \frac{-tr(J) + \sqrt{tr(J)^2 - 4det(J)}}{2\det(J)} = \lim_{[L]\to+\infty} \frac{a + k_3[L] + \sqrt{(a+k_3[L])^2 - 4(k_{-4}k_3[L]+b)}}{2(k_{-4}k_3[L]+b)}$$

$$= \lim_{[L]\to+\infty} \frac{k_3[L] + \sqrt{(k_3[L])^2}}{2k_{-4}k_3[L]} = \lim_{[L]\to+\infty} \frac{2k_3[L]}{2k_{-4}k_3[L]} = \frac{1}{k_{-4}}, \tag{D32}$$

where $a = k_{-1} + k_{-3} + k_{-4}$ and $b = k_{-1}k_{-3} + k_{-1}k_{-4}$.

Data availability

No data was used for the research described in the article.

References

[1] R.A. Copeland, D.L. Pompliano, T.D. Meek, Drug–target residence time and its implications for lead optimization, Nat. Rev. Drug Discov. 5 (9) (Sep. 2006) 730–739, https://doi.org/10.1038/nrd2082.

[2] S. R. Hoare, "Analyzing Kinetic Binding Data," in *Assay Guidance Manual*, 2021. [Online]. Available: https://www.ncbi.nlm.nih.gov/books/NBK569501/.

[3] Ó. Díaz, V. Martín, P. Renault, D. Romero, A. Guillamon, J. Giraldo, Allosteric binding cooperativity in a kinetic context, Drug Discov. Today vol. d, no. 2 (2022) 103441, https://doi.org/10.1016/j.drudis.2022.103441.

[4] A. Cornish-Bowden, *Fundamentals of Enzyme Kinetics*, Wiley-Blackwell (1979).

[5] K.A. Johnson, "1 Transient-State Kinetic Analysis of Enzyme Reaction, Pathways" (1992), https://doi.org/10.1016/S1874-6047(08)60019-0.

[6] J.Z. Hearon, Residence times in compartmental systems with and without inputs, Math. Biosci. 55 (3–4) (Aug. 1981) 247–257, https://doi.org/10.1016/0025-5564(81)90098-5.

[7] Y. Plusquellec, G. Houin, Mean residence time in multicompartmental models with time delays, J. Biomed. Eng. 15 (3) (May 1993) 240–246, https://doi.org/10.1016/0141-5425(93)90121-E.

[8] M.W. Hirsch S. Smale R.L. Devaney Differential Equations, Dynamical Systems, and an Introduction to Chaos 3rd ed. 2013 Elsevier 10.1016/C2009-0-61160-0.

[9] J. Guckenheimer and P. Holmes, *Nonlinear Oscillations, Dynamical Systems, and Bifurcations of Vector Fields*, vol. 42. in Applied Mathematical Sciences, vol. 42. New York, NY: Springer New York, 1983. doi: 10.1007/978-1-4612-1140-2.

[10] P. Hartman, *Ordinary Differential Equations*, 2nd ed., SIAM, 2002.

[11] A. Giuliani, The application of principal component analysis to drug discovery and biomedical data, Drug Discov. Today 22 (7) (Jul. 2017) 1069–1076, https://doi.org/10.1016/j.drudis.2017.01.005.

[12] G. Vauquelin, I. Van Liefde, D.C. Swinney, On the different experimental manifestations of two-state 'induced-fit' binding of drugs to their cellular targets, Br. J. Pharmacol. 173 (8) (Apr. 2016) 1268–1285, https://doi.org/10.1111/bph.13445.

[13] A.D. Vogt, E. Di Cera, Conformational selection or Induced Fit? a critical Appraisal of the Kinetic Mechanism, Biochemistry 51 (30) (Jul. 2012) 5894–5902, https://doi.org/10.1021/bi3006913.

[14] M.R. Dowling, S.J. Charlton, Quantifying the association and dissociation rates of unlabelled antagonists at the muscarinic M 3 receptor, Br. J. Pharmacol. 148 (7) (Aug. 2006) 927–937, https://doi.org/10.1038/sj.bjp.0706819.

[15] V. Georgi, A. Dubrovskiy, S. Steigele, A.E. Fernández-Montalván, Considerations for improved performance of competition association assays analysed with the Motulsky–Mahan's 'kinetics of competitive binding' model, Br. J. Pharmacol. 176 (24) (Dec. 2019) 4731–4744, https://doi.org/10.1111/bph.14841.

[16] D. Guo, et al., A two-state model for the kinetics of competitive radioligand binding, Br. J. Pharmacol. 175 (10) (May 2018) 1719–1730, https://doi.org/10.1111/bph.14184.

[17] J.D. Hothersall, et al., Structure-activity Relationships of the Sustained Effects of Adenosine A2A Receptor Agonists Driven by Slow Dissociation Kinetics, Mol. Pharmacol. 91 (1) (Jan. 2017) 25–38, https://doi.org/10.1124/mol.116.105551.

[18] H.J. Motulsky, L.C. Mahan, The kinetics of competitive radioligand binding predicted by the law of mass action, Mol. Pharmacol. 25 (1) (1984 Jan) 1-9.

[19] K. Hashimoto, A.R. Panchenko, Mechanisms of protein oligomerization, the critical role of insertions and deletions in maintaining different oligomeric states, Proc. Natl. Acad. Sci. 107 (47) (Nov. 2010) 20352–20357, https://doi.org/10.1073/pnas.1012999107.

[20] N. Kumari, S. Yadav, Modulation of protein oligomerization: an overview, Prog. Biophys. Mol. Biol. 149 (Dec. 2019) 99–113, https://doi.org/10.1016/j.pbiomolbio.2019.03.003.

[21] H. Schweke, et al., An atlas of protein homo-oligomerization across domains of life, Cell 187 (4) (Feb. 2024) 999–1010.e15, https://doi.org/10.1016/j.cell.2024.01.022.

[22] J. Giraldo, et al., Analysis of the Function of Receptor Oligomers by Operational Models of Agonism, Comprehensive Pharmacology, Elsevier (2022) 337–359, https://doi.org/10.1016/B978-0-12-820472-6.00012-8.

[23] A. J. Ortiz, V. Martín, D. Romero, A. Guillamon, and J. Giraldo, "Time-dependent ligand-receptor binding kinetics and functionality in a heterodimeric receptor model," Biochem. Pharmacol. (May 2024) p. 116299. https://doi.org/10.1016/j.bcp.2024.116299.

[24] C. White, L.J. Bridge, Ligand Binding Dynamics for Pre-dimerised G Protein-coupled Receptor Homodimers: Linear Models and Analytical Solutions, Bull. Math. Biol. 81 (9) (Sep. 2019) 3542–3574, https://doi.org/10.1007/s11538-017-0387-x.

[25] B. Zhou, J. Giraldo, An operational model for GPCR homodimers and its application in the analysis of biased signaling, Drug Discov. Today 23 (9) (Sep. 2018) 1591–1595, https://doi.org/10.1016/j.drudis.2018.04.004.

[26] D. Colquhoun, Binding, gating, affinity and efficacy: the interpretation of structure-activity relationships for agonists and of the effects of mutating receptors, Br. J. Pharmacol. 125 (5) (Nov. 1998) 923–947, https://doi.org/10.1038/sj.bjp.0702164.

[27] G. Milligan, R.J. Ward, S. Marsango, GPCR homo-oligomerization, Curr. Opin. Cell Biol. 57 (Apr. 2019) 40–47, https://doi.org/10.1016/j.ceb.2018.10.007.

[28] X. Rovira, M. Vivó, J. Serra, D. Roche, P. Strange, J. Giraldo, Modelling the interdependence between the stoichiometry of receptor oligomerization and ligand binding for a coexisting dimer/tetramer receptor system, Br. J. Pharmacol. 156 (1) (Jan. 2009) 28–35, https://doi.org/10.1111/j.1476-5381.2008.00031.x.

[29] N.C. Dale, E.K.M. Johnstone, K.D.G. Pfleger, GPCR heteromers: an overview of their classification, function and physiological relevance, Front Endocrinol (lausanne) 13 (Aug. 2022), https://doi.org/10.3389/fendo.2022.931573.

[30] J. Jang, S.-K. Kim, B. Guthrie, W.A. Goddard, Synergic Effects in the Activation of the Sweet Receptor GPCR Heterodimer for Various Sweeteners Predicted using Molecular Metadynamics Simulations, J. Agric. Food Chem. 69 (41) (Oct. 2021) 12250–12261, https://doi.org/10.1021/acs.jafc.1c03779.

[31] H. Kim, et al., Visualization of differential GPCR crosstalk in DRD1-DRD2 heterodimer upon different dopamine levels, Prog. Neurobiol. 213 (Jun. 2022) 102266, https://doi.org/10.1016/j.pneurobio.2022.102266.

[32] J.-P. Changeux, A. Christopoulos, Allosteric Modulation as a Unifying Mechanism for Receptor Function and Regulation, Cell 166 (5) (Aug. 2016) 1084–1102, https://doi.org/10.1016/j.cell.2016.08.015.

[33] L.T. May, K. Leach, P.M. Sexton, A. Christopoulos, Allosteric Modulation of G Protein–Coupled Receptors, Annu. Rev. Pharmacol. Toxicol. 47 (1) (Feb. 2007) 1–51, https://doi.org/10.1146/annurev.pharmtox.47.120505.105159.

[34] D. Roche, D. Gil, J. Giraldo, Mechanistic analysis of the function of agonists and allosteric modulators: reconciling two-state and operational models, Br. J. Pharmacol. 169 (6) (Jul. 2013) 1189–1202, https://doi.org/10.1111/bph.12231.

[35] E.S. O'Brien, et al., A μ-opioid receptor modulator that works cooperatively with naloxone, Nature 631 (8021) (Jul. 2024) 686–693, https://doi.org/10.1038/s41586-024-07587-7.

[36] W.A.C. Burger, et al., Xanomeline displays concomitant orthosteric and allosteric binding modes at the M4 mAChR, Nat. Commun. 14 (1) (Sep. 2023) 5440, https://doi.org/10.1038/s41467-023-41199-5.

[37] K.E. Knockenhauer, R.A. Copeland, The importance of binding kinetics and drug–target residence time in pharmacology, Br. J. Pharmacol. (Jun. 2023), https://doi.org/10.1111/bph.16104.
[38] W.E.A. de Witte, M. Danhof, P.H. van der Graaf, E.C.M. de Lange, In vivo Target Residence Time and Kinetic Selectivity: the Association Rate constant as Determinant, Trends Pharmacol. Sci. 37 (10) (Oct. 2016) 831–842, https://doi.org/10.1016/j.tips.2016.06.008.
[39] G. Vauquelin, Effects of target binding kinetics on in vivo drug efficacy: k off , k on and rebinding, Br. J. Pharmacol. 173 (15) (Aug. 2016) 2319–2334, https://doi.org/10.1111/bph.13504.
[40] D.A. Sykes, L.A. Stoddart, L.E. Kilpatrick, S.J. Hill, Binding kinetics of ligands acting at GPCRs, Mol. Cell. Endocrinol. 485 (Apr. 2019) 9–19, https://doi.org/10.1016/j.mce.2019.01.018.
[41] G. Vauquelin, D. Maes, Induced fit versus conformational selection: from rate constants to fluxes… and back to rate constants, Pharmacol. Res. Perspect. 9 (5) (2021) Oct, https://doi.org/10.1002/prp2.847.
[42] J.R. Lane, L.T. May, R.G. Parton, P.M. Sexton, A. Christopoulos, A kinetic view of GPCR allostery and biased agonism, Nat. Chem. Biol. 13 (9) (Sep. 2017) 929–937, https://doi.org/10.1038/nchembio.2431.
[43] K.A. Johnson, "[61] Rapid kinetic analysis of mechanochemical adenosinetriphosphatases," 1986, pp. 689–690. https://doi.org/10.1016/0076-6879(86)34129-6.
[44] I.H. Segel, *Enzyme Kinetics: Behavior and Analysis of Rapid Equilibrium and Steady-State Enzyme Systems*, Wiley, 1975.
[45] R.A. Copeland, *Enzymes: a Practical Introduction to Structure, Mechanism, and Data Analysis*, 2nd ed., John Wiley & Sons, 2005.
[46] R.A. Copeland, *Evaluation of Enzyme Inhibitors in Drug Discovery: a Guide for Medicinal Chemists and Pharmacologists*, John Wiley & Sons, 2013.
[47] P.J. Tummino, R.A. Copeland, Residence Time of Receptor−Ligand Complexes and its effect on Biological Function, Biochemistry 47 (20) (May 2008) 5481–5492, https://doi.org/10.1021/bi8002023.
[48] S.R.J. Hoare, N. Pierre, A.G. Moya, B. Larson, Kinetic operational models of agonism for G-protein-coupled receptors, J. Theor. Biol. 446 (Jun. 2018) 168–204, https://doi.org/10.1016/j.jtbi.2018.02.014.
[49] S.R.J. Hoare, P.H. Tewson, A.M. Quinn, T.E. Hughes, L.J. Bridge, Analyzing kinetic signaling data for G-protein-coupled receptors, Sci. Rep. 10 (1) (Jul. 2020) 12263, https://doi.org/10.1038/s41598-020-67844-3.
[50] R. Sexton, M. Fazel, M. Schweiger, S. Pressé, O. Beckstein, Bayesian Nonparametric Analysis of Residence Times for Protein-Lipid Interactions in Molecular Dynamics Simulations, J. Chem. Theory Comput. 21 (8) (2025 Apr 22) 4203–4220. https://doi.org/10.1021/acs.jctc.4c01522.
[51] S.R.J. Hoare, Receptor binding kinetics equations: Derivation using the Laplace transform method, J. Pharmacol. Toxicol. Methods 89 (Jan. 2018) 26–38, https://doi.org/10.1016/j.vascn.2017.08.004.